

# A Taxonomy of Loss Functions for Stochastic Optimal Control

Carles Domingo-Enrich<sup>1</sup>

<sup>1</sup>Microsoft Research New England\*

October 29, 2024

## Abstract

Stochastic optimal control (SOC) aims to direct the behavior of noisy systems and has widespread applications in science, engineering, and artificial intelligence. In particular, reward fine-tuning of diffusion and flow matching models and sampling from unnormalized methods can be recast as SOC problems. A recent work has introduced Adjoint Matching [Domingo-Enrich et al., 2024], a loss function for SOC problems that vastly outperforms existing loss functions in the reward fine-tuning setup. The goal of this work is to clarify the connections between all the existing (and some new) SOC loss functions. Namely, we show that SOC loss functions can be grouped into classes that share the same gradient in expectation, which means that their optimization landscape is the same; they only differ in their gradient variance. We perform simple SOC experiments to understand the strengths and weaknesses of different loss functions.

## 1 Introduction

Stochastic optimal control (SOC) focuses on guiding the behavior of a system affected by randomness to minimize a specified cost function. This approach has diverse applications across various fields in science and engineering, such as simulating rare events in molecular dynamics [Hartmann et al., 2014, Hartmann and Schütte, 2012, Zhang et al., 2014, Holdijk et al., 2023], finance and economics [Pham, 2009, Fleming and Stein, 2004], stochastic filtering and data assimilation [Mitter, 1996, Reich, 2019], nonconvex optimization [Chaudhari et al., 2018], and power systems and energy markets [Belloni et al., 2016, Powell and Meisel, 2016]. It is also widely used in robotics [Theodorou et al., 2011, Gorodetsky et al., 2018]. Additionally, stochastic optimal control has significantly influenced related areas like mean-field games [Carmona et al., 2018], optimal transport [Villani, 2003, 2008], backward stochastic differential equations (BSDEs) [Carmona, 2016], and large deviations [Feng and Kurtz, 2006].

Within machine learning, a relevant and recent application of SOC is performing reward fine-tuning of diffusion and flow matching models [Domingo-Enrich et al., 2024, Uehara et al., 2024]. Reward fine-tuning is a task in which we are given access to a pretrained generative model that generates  $p_{\text{base}}$  and a reward model  $r$ , and we want to modify the pretrained model so that it generates  $p^*(x) \propto p_{\text{base}}(x) \exp(r(x))$ . When the model generates discrete data, such as in large language models, the way to achieve this is through KL-regularized reinforcement learning (RL) [Ziegler et al.,

---

\*Work done partially while at Meta FAIR.

2020, Stiennon et al., 2020, Ouyang et al., 2022, Bai et al., 2022], and the default method is proximal policy optimization (PPO; Schulman et al. [2017]). Since SOC is equivalent to KL-regularized RL for systems with continuous-time trajectories described by stochastic differential equations (see e.g. [Domingo-Enrich et al., 2024, App. C]), any classical KL-regularized RL algorithms can be translated to an SOC algorithm. However, SOC problems have a distinctive feature with respect to classical KL-regularized RL ones: the reward model  $r(x)$  is differentiable because its input is continuous. Exploiting this feature is critical to obtain high-performing deep learning SOC algorithms: [Uehara et al., 2024, Tab. 1,2,3] shows that even a non-state-of-the-art SOC-native algorithm clearly outperforms PPO with KL regularization.

The state-of-the-art SOC (and overall) method for diffusion and flow reward fine-tuning is Adjoint Matching [Domingo-Enrich et al., 2024]. In fact, Adjoint Matching is the only SOC-based reward fine-tuning algorithm that outperforms alternative fine-tuning algorithms such as DRaFT [Clark et al., 2024] and ReFL [Xu et al., 2023], and does so by a big margin (see [Domingo-Enrich et al., 2024, Tab. 2, Fig. 5]). Their work also claims that a particular noise schedule must be used when fine-tuning such models, denoted as the memoryless noise schedule, regardless of the noise schedule that one intends to use at inference time.

These recent developments beg for a systematic overview and comparison of all deep learning methods for SOC problems, both at a theoretical and empirical level. It is critical to understand the strengths and weaknesses of each approach in order to use the appropriate method for each setting. To this end, the contributions of our paper are as follows:

- We review existing SOC loss functions (Subsec. 3.1) and introduce three novel SOC loss functions (Subsec. 3.2): the Work-SOCM loss, the Cost-SOCM loss, and the Unweighted SOCM loss.
- In Sec. 4, we group SOC loss functions into classes that share the same gradient in expectation, which means that their optimization landscape and convergence properties are the same; they only differ in their gradient variance. This results in a taxonomy of loss functions, which we summarize in Figure 1.
- We test the SOC loss functions on a few simple SOC problems that capture relevant features of different practical SOC problems (high dimensions, large costs, multimodality). We observe that despite methods sharing the same gradient in expectation, their convergence speed may differ dramatically due to the gradient variance of each. We also see that different features of the SOC problem favor particular loss functions.

**Related work** The literature on solving stochastic optimal control problems is rich and storied, starting in the 1950s with the work of Richard Bellman [Bellman, 1957], that introduced the Hamilton-Jacobi-Bellman (HJB) equation, a partial differential equation (PDE) whose solution determines the optimal control. For low-dimensional control problems ( $d \leq 3$ ), it is possible to grid the domain and use a numerical PDE solver to find a solution to the HJB equation [Bonnans et al., 2004, Ma and Ma, 2020, Jensen and Smears, 2013, Debrabant and Jakobsen, 2013, Carlini et al., 2020]. To tackle high dimensional problems, works starting in the 2000s designed methods based on forward-backward stochastic differential equations (FBSDEs), initially using least-squares Monte Carlo (see Pham [2009, Chapter 3], and Gobet [2016], Gobet et al. [2005], Zhang et al. [2004]). E et al. [2017], Han et al. [2018] used neural networks to solve SOC problems, leveraging FBSDEs as well. Ever since, a lot of deep learning methods to solve SOC problems have been proposed. We discuss and cite individual methods in Subsec. 3.1, and direct the reader to Domingo-Enrich et al. [2023] and Nüsken and Richter [2021] for more extensive reviews of the related work in this area.

## 2 The stochastic optimal control problem

We consider the control-affine problem

$$\min_{u \in \mathcal{U}} \mathbb{E} \left[ \int_0^T \left( \frac{1}{2} \|u(X_t^u, t)\|^2 + f(X_t^u, t) \right) dt + g(X_T^u) \right], \quad (1)$$

$$\text{where } dX_t^u = (b(X_t^u, t) + \sigma(t)u(X_t^u, t)) dt + \sqrt{\lambda} \sigma(t) dB_t, \quad X_0^u \sim p_0. \quad (2)$$

and where  $X_t^u \in \mathbb{R}^d \rightarrow \mathbb{R}^d$  is the state,  $u : \mathbb{R}^d \times [0, T]$  is the feedback control and belongs to the set of admissible controls  $\mathcal{U}$ ,  $f : \mathbb{R}^d \times [0, T] \rightarrow \mathbb{R}$  is the state cost,  $g : \mathbb{R}^d \rightarrow \mathbb{R}$  is the terminal cost,  $b : \mathbb{R}^d \times [0, T] \rightarrow \mathbb{R}^d$  is the base drift, and  $\sigma : [0, T] \rightarrow \mathbb{R}^{d \times d}$  is the invertible diffusion coefficient, and  $B = (B_t)_{t \geq 0}$  is a Brownian motion. The objective in equation (1) is known as the control objective.

The *cost functional* is the expected future cost starting from state  $x$  at time  $t$ , using the control  $u$ :

$$J(u; x, t) := \mathbb{E}_X \left[ \int_t^1 \left( \frac{1}{2} \|u(X_s, s)\|^2 + f(X_s, s) \right) ds + g(X_1) \mid X_t = x \right]. \quad (3)$$

From here, the *value function* is the optimal value of the cost functional<sup>1</sup>:

$$V(x, t) := \min_{u \in \mathcal{U}} J(u; x, t) = J(u^*; x, t),$$

where  $u^*$  is the *optimal control*, i.e., minimizer of (1). Furthermore, a classical result is that the value function can be expressed in terms of the *uncontrolled* base process  $p^{\text{base}}$  (Kappen [2005], see Domingo-Enrich et al. 2023, Eq. 8, App. B for a self-contained proof):

$$V(x, t) = -\log \mathbb{E}_X \left[ \exp \left( - \int_t^1 f(X_s, s) ds - g(X_1) \right) \mid X_t = x \right],$$

where  $X$  denotes the uncontrolled process (the process with  $u = 0$ ). A useful expression for the optimal control is that it is related to the gradient of the value function (see e.g. Domingo-Enrich et al. 2023, App. B):

$$u^*(x, t) = -\sigma(t)^\top \nabla_x V(x, t) = -\sigma(t)^\top \nabla_x J(u^*, x, t).$$

Solving the SOC problem involves finding the optimal control. The control is parameterized using a neural network. Hence, algorithms are associated to training loss functions. All the loss functions that we study can be optimized using a common algorithmic framework, which we describe in Algorithm 1. Essentially, we refer the reader to Nüsken and Richter [2021], which introduced this perspective and named such methods *Iterative Diffusion Optimization* (IDO) techniques.

---

<sup>1</sup>Note that there is a slight difference in terminology between SOC and reinforcement learning, where our cost functional is referred to as the state value function and our value function is the optimal state value function in RL.

---

**Algorithm 1** Iterative Diffusion Optimization (IDO) algorithms for stochastic optimal control

---

**Input:** Number of iterations  $N$ , batch size  $m$ , number of time steps  $K$ , initial control parameters  $\theta_0$ , loss function  $\mathcal{L}$

**for**  $n \in \{0, \dots, N - 1\}$  **do**

    Simulate  $m$  trajectories  $X^{u_{\theta_n}, i}$  of the process  $X^{u_{\theta_n}}$  controlled by  $u_{\theta_n}$ , e.g., using Euler-Maruyama updates

**if**  $\mathcal{L}$  is not Discrete Adjoint Loss **then** detach the  $m$  trajectories from the computational graph, so that gradients do not backpropagate;

    Compute an  $m$ -sample Monte Carlo approximation  $\frac{1}{m} \sum_{i=1}^m \mathcal{L}(u_{\theta_n}; X^{u_{\theta_n}, i})$  of the expected loss  $\mathbb{E}_{X^{u_{\theta_n}}} \mathcal{L}(u_{\theta_n}; X^{u_{\theta_n}})$

    Compute the gradient  $\nabla_{\theta} \left( \frac{1}{m} \sum_{i=1}^m \mathcal{L}(u_{\theta_n}; X^{u_{\theta_n}, i}) \right)$

    Obtain  $\theta_{n+1}$  with via an Adam update on  $\theta_n$  (or another stochastic algorithm)

**end**

**Output:** Learned control  $u_{\theta_N}$

---

### 3 Loss functions for stochastic optimal control

In this section, we review existing loss functions for stochastic optimal control (Subsec. 3.1), and we introduce three new loss functions, providing theoretical guarantees for each of them (Subsec. 3.2). Unless otherwise indicated, we let  $\bar{u} = \text{stopgrad}(u)$ , which means that the gradients of  $\bar{u}$  with respect to the parameters  $\theta$  of the control  $u$  are artificially set to zero. Some losses admit variants base on the Sticking the Landing (STL) trick (Roeder et al. [2017], [Zhou et al., 2021, Sec. 2.2.3] see App. B), a variance reduction technique that yields zero variance estimators when trajectories are sampled using the optimal control. The STL variants correspond to additional terms that we indicate in blue: removing those terms results in the basic loss function.

#### 3.1 Existing loss functions

**The adjoint method** The adjoint method utilizes the following objective, which is a Monte Carlo estimate of the control objective (1):

$$\mathcal{L}(u; X^u) := \int_0^T \left( \frac{1}{2} \|u(X_t^u, t)\|^2 + f(X_t^u, t) \right) dt + g(X_T^u). \quad (4)$$

The goal is to compute the gradient of  $\mathcal{L}(u; X)$  with respect to the control parameters  $\theta$ .

For optimize the objective (4), two main strategies are used. The *Discrete Adjoint* method follows a “discretize-then-differentiate” approach, retaining the numerical solver in memory for direct differentiation [Han and E, 2016, Bierkens and Kappen, 2014, Chen et al., 2016]. This can be memory-intensive, often requiring gradient checkpointing to reduce usage.

The *Continuous Adjoint* method, however, leverages the continuous nature of SDEs to analytically derive the gradient of the control objective with respect to intermediate states  $X_t$ . This is represented by an adjoint ODE, following a “differentiate-then-discretize” approach [Pontryagin, 1962, Chen et al., 2018, Li et al., 2020]. The adjoint state is defined as:

$$\begin{aligned} a(t; X^u, u) &:= \nabla_{X_t} \left( \int_t^T \left( \frac{1}{2} \|u(X_{t'}^u, t')\|^2 + f(X_{t'}^u, t') \right) dt' + g(X_1^u) \right), \\ \text{where } X^u &\text{ solves } dX_t^u = (b(X_t^u, t) + \sigma(t)u(X_t^u, t)) dt + \sigma(t)dB_t. \end{aligned}$$

This implies that  $\mathbb{E}_{X^u} [a(t; X^u, u) | X_t^u = x] = \nabla_x J(u; x, t)$ , where  $J$  is the cost functional (3).

The adjoint state evolves according to the dynamics<sup>2</sup>:

$$da(t; X^u, u) = - \left[ \left( \nabla_{X_t^u} (b(X_t^u, t) + \sigma(t)u(X_t^u, t)) \right)^\top a(t; X^u, u) + \nabla_{X_t^u} \left( f(X_t^u, t) + \frac{1}{2} \|u(X_t^u, t)\|^2 \right) \right] dt - \nabla_x \bar{u}(X_t^u, t) dB_t, \quad (5)$$

$$a(T; X^u, u) = \nabla g(X_T^u). \quad (6)$$

The adjoint state is solved backward in time, and once obtained over the interval  $t \in [0, 1]$ , the gradient of  $\mathcal{L}(u; \mathbf{X})$  with respect to  $\theta$  is computed by integrating over the entire time span:

$$\frac{d\mathcal{L}}{d\theta} = \frac{1}{2} \int_0^T \frac{\partial}{\partial \theta} \|u(X_t^{\bar{u}}, t)\|^2 dt + \int_0^T \frac{\partial u(X_t^{\bar{u}}, t)}{\partial \theta}^\top \sigma(t)^\top a(t; X^{\bar{u}}, \bar{u}) dt, \quad \bar{u} = \text{stopgrad}(u), \quad (7)$$

The first term in (7) corresponds to the direct partial derivative of  $\mathcal{L}$  with respect to  $\theta$ , and the second term captures the derivative through the sampled trajectory  $X^u$  [Domingo-Enrich et al., 2024, Prop. 6].

Both discrete and continuous adjoint methods converge to the same gradient as the numerical solver step size approaches zero, and scale efficiently to high-dimensional problems. Despite their efficacy in optimizing neural ODE/SDEs, they can be unstable in practice due to the non-convexity of the problem [Mohamed et al., 2020, Suh et al., 2022, Domingo-Enrich et al., 2023].

An alternative way to derive the loss (4) is as the KL divergence or relative entropy between  $\mathbb{P}^u$ , the distribution over trajectories induced by the control  $u$ , and  $\mathbb{P}^{u^*}$ , the distribution over trajectories induced by the control  $u^*$ . That is,  $\mathcal{L}(u; X^u) = \mathbb{E}_{\mathbb{P}^{u^*}} [\log \frac{d\mathbb{P}^u}{d\mathbb{P}^{u^*}}]$ , which is why some works [Nüsken and Richter, 2021] refer to this loss as the relative entropy loss. See Domingo-Enrich et al. 2024, Sec. 5.1 for more details on the adjoint method.

**Adjoint Matching** Adjoint Matching was introduced in Domingo-Enrich et al. 2024, Sec. 5.2, and it is an improvement over the Continuous Adjoint method that is based on two observations. The first one is that the gradient of the Continuous Adjoint loss in (7) is equal to the gradient of the basic Adjoint Matching loss, defined as:

$$\mathcal{L}_{\text{Basic-Adj-Match}}(u; X^{\bar{u}}) := \frac{1}{2} \int_0^T \|u(X_t^{\bar{u}}, t) + \sigma(t)^\top a(t; X^{\bar{u}}, \bar{u})\|^2 dt, \quad \bar{u} = \text{stopgrad}(u), \quad (8)$$

The second observation is that the adjoint ODE (5)-(6) can be simplified, giving rise to the lean adjoint ODE, which is as follows:

$$d\tilde{a}(t; X^{\bar{u}}, \bar{u}) = -(\tilde{a}(t; X^{\bar{u}}, \bar{u})^\top \nabla_x b(X_t^{\bar{u}}, t) + \nabla_x f(X_t^{\bar{u}}, t)) dt - \nabla_x \bar{u}(X_t^{\bar{u}}, t) dB_t, \quad (9)$$

$$\tilde{a}(T; X^{\bar{u}}, \bar{u}) = \nabla_x g(X_T^{\bar{u}}). \quad (10)$$

And then, the Adjoint Matching loss is analogous to the basic Adjoint Matching loss, replacing the adjoint state  $a(t; X^{\bar{u}}, \bar{u})$  by the lean adjoint state  $\tilde{a}(t; X^{\bar{u}})$ :

$$\mathcal{L}_{\text{Adj-Match}}(u; X^{\bar{u}}) := \frac{1}{2} \int_0^T \|u(X_t^{\bar{u}}, t) + \sigma(t)^\top \tilde{a}(t; X^{\bar{u}})\|^2 dt, \quad \bar{u} = \text{stopgrad}(u). \quad (11)$$

While the gradients of the expected losses  $\mathbb{E}[\mathcal{L}_{\text{Basic-Adj-Match}}]$  and  $\mathbb{E}[\mathcal{L}_{\text{Adj-Match}}]$  are not equal, both losses have the same theoretical guarantees. Namely, the only critical point of the expected losses is the optimal control. A critical point of a loss  $\mathcal{L}$  is a control  $u$  such that  $\frac{\delta}{\delta u} \mathcal{L}(u) = 0$ , where  $\frac{\delta}{\delta u} \mathcal{L}$  denotes the first variation of the functional  $\mathcal{L}$ . This guarantee provides the theoretical grounding for gradient-based optimization algorithms to optimize  $\mathbb{E}[\mathcal{L}_{\text{Basic-Adj-Match}}]$  and  $\mathbb{E}[\mathcal{L}_{\text{Adj-Match}}]$ . See Domingo-Enrich et al. 2024, App. E.2, E.3 for the proofs.

<sup>2</sup>Here, the Jacobian matrix  $\nabla_x v(x)$  is defined as  $(\nabla_x v(x))_{ij} = \frac{\partial v_i(x)}{\partial x_j}$ .

**The REINFORCE losses** Policy gradient methods, and in particular the archetypal REINFORCE method, are classical RL algorithms that also have analogs in stochastic optimal control, through the connection between stochastic optimal control and KL-regularized reinforcement learning (see [Domingo-Enrich et al. 2024](#), App. C). The regular REINFORCE loss, which we derive in [Prop. 4](#), reads:

$$\begin{aligned} \mathcal{L}_{\text{RF}}(u; X^{\bar{u}}) &:= \frac{1}{2} \int_0^T \|u(X_t^{\bar{u}}, t)\|^2 dt \\ &\quad + \left( \int_0^T \left( \frac{1}{2} \|\bar{u}(X_t^{\bar{u}}, t)\|^2 + f(X_t^{\bar{u}}, t) \right) dt + g(X_T^{\bar{u}}) \right) \times \int_0^T \langle u(X_t^{\bar{u}}, t), dB_t \rangle, \end{aligned} \quad (12)$$

while the expression for the REINFORCE loss that uses only future rewards is as follows:

$$\begin{aligned} \mathcal{L}_{\text{RFFR}}(u; X^{\bar{u}}) &:= \frac{1}{2} \int_0^T \|u(X_t^{\bar{u}}, t)\|^2 dt \\ &\quad + \int_0^T \left( \int_t^T \left( \frac{1}{2} \|\bar{u}(X_s^{\bar{u}}, s)\|^2 + f(X_s^{\bar{u}}, s) \right) ds + g(X_T^{\bar{u}}) \right) \langle u(X_t^{\bar{u}}, t), dB_t \rangle, \end{aligned} \quad (13)$$

**The cross-entropy loss** The cross-entropy loss is defined as the Kullback-Leibler divergence between  $\mathbb{P}^{u^*}$  and  $\mathbb{P}^u$ , i.e., flipping the order of the two measures:  $\mathbb{E}_{\mathbb{P}^{u^*}} \left[ \log \frac{d\mathbb{P}^{u^*}}{d\mathbb{P}^u} \right]$ . For an arbitrary  $v \in \mathcal{U}$ , this loss is equivalent to the following one (see e.g. [\[Domingo-Enrich et al., 2023, Prop. B.6\(i\)\]](#)):

$$\begin{aligned} \mathcal{L}_{\text{CE}}(u; X^{\bar{u}}) &:= \left( - \int_0^T \langle u(X_t^{\bar{u}}, t), dB_t \rangle - \int_0^T \langle u(X_t^{\bar{u}}, t), \bar{u}(X_t^{\bar{u}}, t) \rangle dt \right. \\ &\quad \left. + \frac{1}{2} \int_0^T \|u(X_t^{\bar{u}}, t)\|^2 dt \right) \times \alpha(\bar{u}, X^{\bar{u}}, B), \end{aligned} \quad (14)$$

$$\text{where } \alpha(\bar{u}, X^{\bar{u}}, B) = \exp \left( - \left( \int_0^T \left( \frac{1}{2} \|\bar{u}(X_t^{\bar{u}}, t)\|^2 + f(X_t^{\bar{u}}, t) \right) ds + g(X_T^{\bar{u}}) - \int_0^T \langle \bar{u}(X_t^{\bar{u}}, t), dB_t \rangle \right) \right) \quad (15)$$

The cross-entropy loss has a rich literature [[Hartmann et al., 2017](#), [Kappen and Ruiz, 2016](#), [Rubinstein and Kroese, 2013](#), [Zhang et al., 2014](#)] and has been recently used in applications such as molecular dynamics [[Holdijk et al., 2023](#)]. However, the variance of the factor  $\alpha$  blows up when  $f$  or  $g$  are large or the dimension is high, which hinders the practical applicability of the loss in large-scale settings.

**Variance and log-variance losses** The *variance* and the *log-variance losses* are defined as  $\tilde{\mathcal{L}}_{\text{Var}_{\bar{u}}}(u) = \text{Var}_{\mathbb{P}^{\bar{u}}} \left( \frac{d\mathbb{P}^{u^*}}{d\mathbb{P}^{\bar{u}}} \right)$  and  $\tilde{\mathcal{L}}_{\text{Var}_{\bar{u}}}^{\log}(u) = \text{Var}_{\mathbb{P}^{\bar{u}}} \left( \log \frac{d\mathbb{P}^{u^*}}{d\mathbb{P}^{\bar{u}}} \right)$  whenever  $\mathbb{E}_{\mathbb{P}^{\bar{u}}} \left| \frac{d\mathbb{P}^{u^*}}{d\mathbb{P}^{\bar{u}}} \right| < +\infty$  and  $\mathbb{E}_{\mathbb{P}^{\bar{u}}} \left| \log \frac{d\mathbb{P}^{u^*}}{d\mathbb{P}^{\bar{u}}} \right| < +\infty$ , respectively. Define

$$\tilde{Y}_T^{u, \bar{u}} = - \int_0^T \langle u(X_t^{\bar{u}}, t), \bar{u}(X_t^{\bar{u}}, t) \rangle dt - \int_0^T f(X_t^{\bar{u}}, t) dt - \int_0^T \langle u(X_t^{\bar{u}}, t), dB_t \rangle + \frac{1}{2} \int_0^T \|u(X_t^{\bar{u}}, t)\|^2 dt \quad (16)$$

Then,  $\tilde{\mathcal{L}}_{\text{Var}_{\bar{u}}}$  and  $\tilde{\mathcal{L}}_{\text{Var}_{\bar{u}}}^{\log}$  are equivalent, respectively, to the following losses (see e.g. [\[Domingo-Enrich et al., 2023, Prop. B.6\(i\)\]](#)):

$$\mathcal{L}_{\text{Var}_{\bar{u}}}(u) := \text{Var} \left( \exp \left( \tilde{Y}_T^{u, \bar{u}} - g(X_T^{\bar{u}}) \right) \right), \quad (17)$$

$$\mathcal{L}_{\text{Var}_{\bar{u}}}^{\log}(u) := \text{Var} \left( \tilde{Y}_T^{u, \bar{u}} - g(X_T^{\bar{u}}) \right), \quad (18)$$

The variance and log-variance losses were introduced by [Nüsken and Richter \[2021\]](#). Unlike for the cross-entropy loss, the choice of the control  $\bar{u}$  does lead to different losses. When using  $\mathcal{L}_{\text{Var}_{\bar{u}}}$  or  $\mathcal{L}_{\text{Var}_{\bar{u}}}^{\log}$  in [Algorithm 1](#), the variance is computed across the  $m$  trajectories in each batch. Note that when  $f, g$  are large,  $\mathcal{L}_{\text{Var}_{\bar{u}}}$  is very large and has itself very large variance, which causes issues.

**Moment loss** The moment loss is defined as

$$\mathcal{L}_{\text{Mom}_{\bar{u}}}(u, y_0) = (\tilde{Y}_T^{u, \bar{u}} + y_0 - g(X_T^{\bar{u}}))^2, \quad (19)$$

where  $\tilde{Y}_T^{u, \bar{u}}$  is defined in (16). Note the similarity with the log-variance loss (18); the optimal value of  $y_0$  for a fixed  $u$  is  $y_0^* = \mathbb{E}[g(X_T^{\bar{u}}) - \tilde{Y}_T^{u, \bar{u}}]$ , and plugging this into the expectation of (19) yields exactly the log-variance loss. The moment loss was introduced by Hartmann et al. [2019, Section III.B], generalizing the FBSDE method pioneered by E et al. [2017], Han et al. [2018], which corresponds to setting  $\bar{u} = 0$ .

**Stochastic optimal control matching (SOCM) loss** This loss, introduced by Domingo-Enrich et al. [2023], is formally similar to the Continuous Adjoint loss, in that the control  $u(x, t)$  is trained to approximate a certain vector field. The SOCM is as follows:

$$\mathcal{L}_{\text{SOCM}}(u, M) := \int_0^T \left\| u(X_t^{\bar{u}}, t) + \sigma(t)^\top \omega(t, \bar{u}, X_t^{\bar{u}}, B, M_t) \right\|^2 dt \times \alpha(\bar{u}, X_t^{\bar{u}}, B), \quad (20)$$

where  $\alpha(\bar{u}, X_t^{\bar{u}}, B)$  is defined in (15), and

$$\begin{aligned} \omega(t, \bar{u}, X_t^{\bar{u}}, B, M_t) &= \int_t^T M_t(s) \nabla_x f(X_s^{\bar{u}}, s) ds + M_t(T) \nabla g(X_T^v) \\ &\quad - \int_t^T (M_t(s) \nabla_x b(X_s^v, s) - \partial_s M_t(s)) (\sigma^{-1})^\top(s) \bar{u}(X_s^{\bar{u}}, s) ds \\ &\quad - \int_t^T (M_t(s) \nabla_x b(X_s^v, s) - \partial_s M_t(s)) (\sigma^{-1})^\top(s) dB_s, \end{aligned} \quad (21)$$

and  $M$  satisfy the following assumption:

**Assumption 1.** For each  $t \in [0, T]$ ,  $M_t : [t, T] \rightarrow \mathbb{R}^{d \times d}$  is an arbitrary matrix-valued differentiable function such that  $M_t(t) = \text{Id}$ . More generally, we can take  $M_t$  such that for any  $s \in [t, T]$ ,  $M_t(s)$  depends on the trajectory  $X^{\bar{u}}$  up to time  $s$ .

Observe that  $u(x, t)$  is trained to approximate

$$\frac{-\sigma(t)^\top \mathbb{E}[\omega(t, \bar{u}, X_t^{\bar{u}}, B, M_t) \alpha(\bar{u}, X_t^{\bar{u}}, B) | X_t^{\bar{u}} = x]}{\mathbb{E}[\alpha(\bar{u}, X_t^{\bar{u}}, B) | X_t^{\bar{u}} = x]}. \quad (22)$$

Leveraging the path-wise reparameterization trick ([Domingo-Enrich et al., 2023, Prop. 1], Thm. 4, Cor. 2), one sees that for any  $\bar{u} \in \mathcal{U}$  and  $M$  satisfying Assumption 1, the term in (22) is equal to the optimal control  $u^*(x, t)$ . Minimizing the loss  $\mathcal{L}_{\text{SOCM}}$  with respect to  $M$  serves the purpose of minimizing the variance of the target vector field, making it easier and faster to learn. This is the reason the SOCM loss outperforms all other losses in simple experiments (Sec. 5). On the flip side, like for the cross entropy loss, the variance blowup of the factor  $\alpha$  makes this loss impractical at large scale.

**SOCM-Adjoint loss** The SOCM-Adjoint loss, introduced by Domingo-Enrich et al. [2023], is of this form:

$$\mathcal{L}_{\text{SOCM-Adj}}(u) := \int_0^T \left\| u(X_t^{\bar{u}}, t) + \sigma(t)^\top \tilde{a}(t, X_t^{\bar{u}}) \right\|^2 dt \times \alpha(\bar{u}, X_t^{\bar{u}}, B), \quad (23)$$

where  $\alpha(\bar{u}, X_t^{\bar{u}}, B)$  is the importance weight defined in (15), and  $\tilde{a}(t, X_t^{\bar{u}})$  is the solution of the lean adjoint ODE (9)-(10). Remark that the only difference between the SOCM-Adjoint loss and the Adjoint Matching loss is the importance weight  $\alpha(\bar{u}, X_t^{\bar{u}}, B)$ ; the variance of this factor blows up when  $f$  or  $g$  are large or the dimension is high, which hinders the practical applicability of the loss in large-scale settings. Observe also that  $u(x, t)$  is trained to approximate the vector field  $\frac{-\sigma(t)^\top \mathbb{E}[\tilde{a}(t, X_t^v) \alpha(\bar{u}, X_t^{\bar{u}}, B) | X_t^{\bar{u}} = x]}{\mathbb{E}[\alpha(\bar{u}, X_t^{\bar{u}}, B) | X_t^{\bar{u}} = x]}$ , which is equal to the optimal control  $u^*(x, t)$ , because  $\frac{\mathbb{E}[\tilde{a}(t, X_t^{\bar{u}}) \alpha(\bar{u}, X_t^{\bar{u}}, B) | X_t^{\bar{u}} = x]}{\mathbb{E}[\alpha(\bar{u}, X_t^{\bar{u}}, B) | X_t^{\bar{u}} = x]} = \nabla V(x, t)$  for any  $v \in \mathcal{U}$ .

### 3.2 New loss functions

**Work-SOCM loss** In this loss, the control  $u$  is also trained to approximate the vector field  $-\sigma(t)^\top \mathbb{E}[\tilde{\xi}(t, X^{\bar{u}}, B, M_t) | X_t^{\bar{u}} = x]$ :

$$\mathcal{L}_{\text{Work-SOCM}}(u, M) := \int_0^T \|u(X_t^{\bar{u}}, t) + \sigma(t)^\top \tilde{\xi}(t, X^{\bar{u}}, B, M_t)\|^2 dt, \quad \bar{u} = \text{stopgrad}(u), \quad (24)$$

where

$$\begin{aligned} \tilde{\xi}(t, X^v, B, M_t) &= \int_t^T M_t(s) \nabla_x f(X_s^v, s) ds + M_t(T) \nabla g(X_T^v) \\ &\quad + \left( \int_t^T f(X_s^v, s) ds + g(X_T^v) \right) \times \left( \int_t^T (M_t(s) \nabla_x b(X_s^v, s) - \partial_s M_t(s)) (\sigma^{-1})^\top(s) dB_s \right). \end{aligned}$$

and  $M$  is a family of matrix-valued functions that satisfies [Assumption 1](#). That is,  $u(x, t)$  is trained to approximate  $-\sigma(t)^\top \mathbb{E}[\tilde{\xi}(t, X^{\bar{u}}, B, M_t) | X_t^{\bar{u}} = x]$ . The following proposition connects the Work-SOCM loss to the Adjoint Matching loss, which allows us to deduce theoretical guarantees for the former.

**Proposition 1.** *The gradients of the losses  $\mathcal{L}_{\text{Adj-Match}}$  and  $\mathcal{L}_{\text{Work-SOCM}}$  are equal in expectation, and in particular, for any  $x \in \mathbb{R}^d$ ,  $t \in T$ , and  $M$  fulfilling [Assumption 1](#), we have that*

$$\mathbb{E}[\tilde{a}(t, X^{\bar{u}}) | X_t^{\bar{u}} = x] = \mathbb{E}[\tilde{\xi}(t, X^{\bar{u}}, B, M_t) | X_t^{\bar{u}} = x] = \mathbb{E}[\nabla_{X_t} \left( \int_t^T f(X_s, s) ds + g(X_T) \right) \frac{d\mathbb{P}^v}{d\mathbb{P}}(X) | X_t = x]. \quad (25)$$

Hence, the only critical point of the loss  $\mathcal{L}_{\text{Work-SOCM}}$  is the optimal control  $u^*$ .

The reason for the term *work* in the name of this loss is that equation (25) involves the work functional  $\mathcal{W}(X, t) = \int_t^T f(X_s, s) ds + g(X_T)$ .

**Cost-SOCM loss** The control  $u$  is trained to approximate the vector field  $-\sigma(t)^\top \mathbb{E}[\xi(t, X^{\bar{u}}, B, M_t) | X_t^{\bar{u}} = x]$ :

$$\mathcal{L}_{\text{Cost-SOCM}}(u, M) := \int_0^T \|u(X_t^{\bar{u}}, t) + \sigma(t)^\top \xi(t, \bar{u}, X^{\bar{u}}, B, M_t)\|^2 dt, \quad \bar{u} = \text{stopgrad}(u), \quad (26)$$

where

$$\begin{aligned} \xi(t, \bar{u}, X^{\bar{u}}, B, M_t) &= \int_t^T M_t(s) \nabla_x (f(X_s^{\bar{u}}, s) + \frac{1}{2} \|\bar{u}(X_s^{\bar{u}}, s)\|^2) ds + M_t(T) \nabla g(X_T^{\bar{u}}) + \int_t^T M_t(s) \nabla_x \bar{u}(X_s^{\bar{u}}, s) dB_s \\ &\quad - \left( \int_t^T (f(X_s^{\bar{u}}, s) + \frac{1}{2} \|\bar{u}(X_s^{\bar{u}}, s)\|^2) ds + g(X_T^{\bar{u}}) + \int_t^T \bar{u}(X_s^{\bar{u}}, s) dB_s \right) \\ &\quad \times \left( \int_t^T (M_t(s) \nabla_x (b(X_s^{\bar{u}}, s) + \sigma(s) \bar{u}(X_s^{\bar{u}}, s)) - \partial_s M_t(s)) (\sigma^{-1})^\top(s) dB_s \right), \end{aligned}$$

and  $M$  is a family of matrix-valued functions that satisfies [Assumption 1](#). As shown by [Prop. 2](#), the expectation  $\mathbb{E}[\xi(t, X^{\bar{u}}, B, M_t) | X_t^{\bar{u}} = x]$  is equal to the gradient of the expected cost functional  $\nabla_x J(\bar{u}; x, t)$ , which means that in expectation,  $\mathcal{L}_{\text{Cost-SOCM}}$  has the same gradients as  $\mathcal{L}_{\text{Cont-Adj}}$ .

**Proposition 2.** *In expectation, the gradients of the loss  $\mathcal{L}_{\text{Cost-SOCM}}$  are equal to the gradients of the continuous adjoint loss  $\mathcal{L}_{\text{Cont-Adj}}$ . In particular, we have that*

$$\mathbb{E}[\xi(t, \bar{u}, X^{\bar{u}}, B, M_t) | X_t^{\bar{u}} = x] = \nabla \mathbb{E} \left[ \int_0^T \left( \frac{1}{2} \|\bar{u}(X_t^{\bar{u}}, t)\|^2 + f(X_t^{\bar{u}}, t) \right) dt + g(X_T^{\bar{u}}) | X_0^{\bar{u}} = x \right].$$

**Unweighted SOCM loss** As implied by its name, the difference between the Unweighted SOCM loss and the SOCM loss is that the former does not include the factor  $\alpha$ :

$$\mathcal{L}_{\text{UW-SOCM}}(u, M) := \int_0^T \|u(X_t^{\bar{u}}, t) + \sigma(t)^\top \omega(t, \bar{u}, X_t^{\bar{u}}, B, M_t)\|^2 dt, \quad \bar{u} = \text{stopgrad}(u). \quad (27)$$

The upside of removing  $\alpha$  is that the gradient variance does not blow up even with large scale problems. The downside is that the theoretical guarantees of this loss are weak:

**Proposition 3.** *For any  $M$ , the optimal control  $u^*$  is a critical point of  $\mathcal{L}_{\text{UW-SOCM}}(\cdot, M)$ .*

**Prop. 3** does not preclude the existence of other critical points beyond  $u^*$ . In fact, from the expression of  $\omega$  (21), we see that if we choose  $M_t$  such that  $M_t(T) = 0$ , the loss becomes underspecified because it has no information about the terminal cost  $g$  (the optimal control for any cost  $g$  is a critical point!). In practice, UW-SOCM is the best-performing algorithm in several experimental settings of [Sec. 5](#), but fails to convergence in other ones.

## 4 A taxonomy of loss functions

The SOC losses presented in [Subsec. 3.1](#) and [Subsec. 3.2](#) are connected to each other in multiple ways. These connections have been partially addressed in those sections, but it is useful for researchers to have a clear, systematic, complete picture of all the losses that are available. [Thm. 1](#) specifies the sets of losses that have equal gradients in expectation, up to numerical errors (see proofs in [App. E](#)).

**Theorem 1** (A taxonomy of SOC losses). *In expectation and in the limit where SDE simulation stepsize goes to zero, the gradients of the following sets of loss functions are equal up to constant factors:*

- *Class I: Discrete Adjoint (4), Continuous Adjoint (8), REINFORCE (12), REINFORCE (future rewards) (13), Cost-SOCM (26).*
- *Class II: Adjoint Matching (11) and Work-SOCM (24).*
- *Class III: SOCM (20), SOCM-Adjoint (23), Cross Entropy (14).*
- *Class IV: Log-variance (18), Moment (19) (if batch size  $\rightarrow \infty$  in the former and  $y_0$  is optimized instantaneously in the latter).*
- *Class V: Variance (17).*
- *Class VI: Unweighted SOCM (27).*

Note that theoretical guarantees proven for a single loss function apply to all the loss functions in the class, because they all share the same gradient in expectation. That allows us to make unified statements about the convergence properties for each class, relying on the theoretical guarantees that we review and claim in [Sec. 3](#).

Loss functions in Class I are explicitly or implicitly optimizing the control objective, or equivalently the KL divergence between  $\mathbb{P}^u$  and  $\mathbb{P}^{u^*}$ , through gradient descent. Even though the control objective is not convex in function space, the only critical point of all these losses is the optimal control. Similarly, loss functions in Class III are optimizing the KL divergence between  $\mathbb{P}^{u^*}$  and  $\mathbb{P}^u$ . This is a strongly convex functional with respect to the control  $u$ , and the only critical point of all these

No differentiability requirements		Base drift, state cost differentiable, terminal cost optionally diff.	Base drift, state & terminal cost differentiable
REINFORCE REINFORCE (future rewards)		<u>Cost-SOCM (+STL)</u>	Discrete Adjoint Continuous Adjoint (+STL)
		<u>Work-SOCM</u>	Adjoint Matching (+STL)
Cross Entropy		SOCM	SOCM-Adjoint
Log-variance Moment	Variance	<u>Unweighted SOCM</u>	

Figure 1: Training losses for stochastic optimal control problems. Losses in blue scale to high-dimensions, while losses in red do not, as the gradient variance blows up exponentially with the dimension. By [Thm. 1](#), losses in the same block (there are five different blocks) are equal in expectation, i.e. taking infinite batch size would yield the same gradient update. Novel losses are underlined, and losses that admit a Sticking The Landing version are identified with the suffix (+STL).

losses is the optimal control. Loss functions in Class II have a single critical point which is the optimal control, but they cannot be regarded as performing gradient-based optimization on any objective functional.

The information in [Thm. 1](#) is summarized in [Figure 1](#). Additionally, the diagram contains information on the losses that require differentiating through the state and terminal costs, those that do not, and those that differentiate the state cost and may or may not differentiate the terminal costs. The latter are SOCM based losses in which the reparameterization matrices  $M$  can be chosen such that  $M_t(T) = 0$  for all  $t \in [0, T]$ , which means that we do not need to evaluate the gradient of  $g$ .

## 5 Simple stochastic optimal control experiments

We benchmark all the loss functions in our taxonomy in [Figure 1](#) on four experimental settings where we have access to the ground truth optimal control, which means that we can compute the control  $L^2$  error incurred by each algorithm throughout training. The settings are QUADRATIC ORNSTEIN UHLENBECK, EASY and HARD, and DOUBLE WELL, EASY and HARD, and LINEAR, and were used in [Domingo-Enrich et al. \[2023\]](#), [Nüsken and Richter \[2021\]](#). The code can be found at <https://github.com/facebookresearch/SOC-matching/tree/deep-Q-learning>.

[Figure 2](#) contains all the plots; errors are averaged using an exponential moving average. The top left subfigure corresponds to an easy setting where all algorithms perform well. The best-performing losses are SOCM and UW-SOCM, which we introduce in [Subsec. 3.2](#). The top right subfigure is on a more challenging setting in which the running cost  $f$  and the terminal cost  $g$  are larger, where losses that do not scale well (those in red in [Figure 1](#)) struggle. Larger costs make these losses fail completely, as gradient variance is too high. UW-SOCM achieves the lowest error.

The middle subfigures are for settings where the optimal process has 1024 modes. Algorithms need to explore all the modes, which is why the control  $L^2$  errors decrease slower than in the

top subfigures, and also the reason why some plots have occasional bounces. In the middle left subfigure, Adjoint Matching achieves the lowest error, and UW-SOCM is the best loss among those for which the error decreases monotonically. In the middle right subfigure, UW-SOCM shows unstable behavior which we attribute to its weak theoretical guarantees (Prop. 3), and the best loss is SOCM. In the bottom figure, SOCM, UW-SOCM, and SOCM-Adjoint perform similarly.

In summary, while SOCM and UW-SOCM are the best loss functions in some settings, they struggle in others. The failure modes of SOCM are high dimensions and high-magnitude cost functions, both of which cause the importance weight  $\alpha$  to have high variance, and one failure mode of UW-SOCM is multimodal problems, as the control fails to converge. In comparison, the performance of Continuous Adjoint and Adjoint Matching is not as good in simple settings such as QUADRATIC OU, EASY and LINEAR, but they behave well across the board. Overall, SOCM-Cost and SOCM-Work have a similar performance, but at a higher computational cost, and the Log-Variance, Variance, Moment and Discrete Adjoint losses perform noticeably worse. Among the losses that converge, the worst ones across the board are the two REINFORCE losses. Thus, our experiments show that the Continuous Adjoint loss and the REINFORCE loss, which have the same gradient according to our taxonomy, have completely different behaviors, and this is due to different gradient variances. In App. G we show additional plots and include more detailed comparisons among different loss functions, and in App. F we include more information about the experiments.

## 6 Conclusion

In this paper, we clarify the connections between existing and new deep learning loss functions to solve SOC problems, which have been recently applied to fine-tune diffusion and flow matching models. In particular, we observe that loss functions can be clustered into classes that share the same gradient in expectation. Qualitatively, all the losses in each class have the same convergence behavior, which we study. Quantitatively, losses within a class have gradient variances of different magnitudes, which translates to different convergence speeds. We compare all the losses on five different synthetic SOC problems.

## References

- Y. Bai, A. Jones, K. Ndousse, A. Askell, A. Chen, N. DasSarma, D. Drain, S. Fort, D. Ganguli, T. Henighan, N. Joseph, S. Kadavath, J. Kernion, T. Conerly, S. El-Showk, N. Elhage, Z. Hatfield-Dodds, D. Hernandez, T. Hume, S. Johnston, S. Kravec, L. Lovitt, N. Nanda, C. Olsson, D. Amodei, T. Brown, J. Clark, S. McCandlish, C. Olah, B. Mann, and J. Kaplan. Training a helpful and harmless assistant with reinforcement learning from human feedback. *arXiv preprint arXiv:2204.05862*, 2022.
- R. Bellman. *Dynamic programming*. Princeton Landmarks in Mathematics. Princeton University Press, Princeton, NJ, 2010., 1957.
- A. Belloni, L. Piroddi, and M. Prandini. A stochastic optimal control solution to the energy management of a microgrid with storage and renewables. In *2016 American Control Conference (ACC)*, pages 2340–2345, 2016.
- J. Bierkens and H. J. Kappen. Explicit solution of relative entropy weighted control. *Systems & Control Letters*, 72:36–43, 2014.

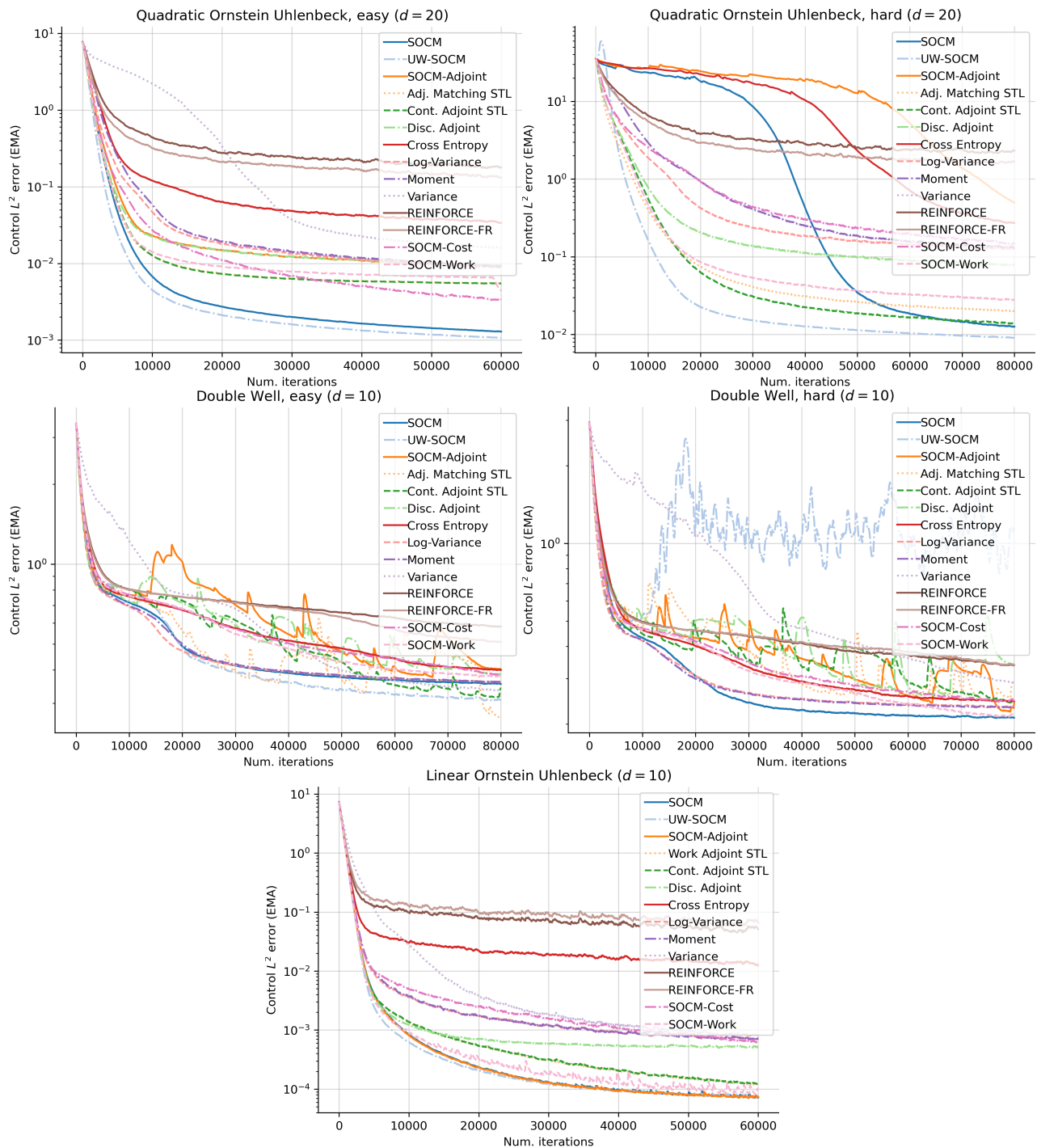


Figure 2: Control  $L^2$  error incurred by each loss function throughout training, on five different settings.

- J. Bonnans, E. Ottenwaelter, and H. Zidani. A fast algorithm for the two dimensional hjb equation of stochastic control. *M2AN. Mathematical Modelling and Numerical Analysis. ESAIM, European Series in Applied and Industrial Mathematics*, 38, 07 2004.
- E. R. Borrell, J. Quer, L. Richter, and C. Schütte. Improving control based importance sampling strategies for metastable diffusions via adapted metadynamics. *arXiv preprint arXiv:2206.06628*, 2022.
- E. Carlini, A. Festa, and N. Forcadel. A semi-Lagrangian scheme for Hamilton–Jacobi–Bellman equations on networks. *SIAM J. Numer. Anal.*, 58(6):3165–3196, 2020.
- R. Carmona. *Lectures on BSDEs, stochastic control, and stochastic differential games with financial applications*, volume 1. SIAM, 2016.
- R. Carmona, F. Delarue, et al. *Probabilistic Theory of Mean Field Games with Applications I-II*. Springer, 2018.
- P. Chaudhari, A. Oberman, S. Osher, S. Soatto, and G. Carlier. Deep relaxation: partial differential equations for optimizing deep neural networks. *Research in the Mathematical Sciences*, 5(3):30, 2018.
- R. T. Q. Chen, Y. Rubanova, J. Bettencourt, and D. K. Duvenaud. Neural ordinary differential equations. In *Advances in Neural Information Processing Systems*, volume 31. Curran Associates, Inc., 2018.
- T. Chen, B. Xu, C. Zhang, and C. Guestrin. Training deep nets with sublinear memory cost. *arXiv preprint arXiv:1604.06174*, 2016.
- K. Clark, P. Vicol, K. Swersky, and D. J. Fleet. Directly fine-tuning diffusion models on differentiable rewards. In *The Twelfth International Conference on Learning Representations*, 2024.
- K. Debrabant and E. R. Jakobsen. Semi-lagrangian schemes for linear and fully non-linear diffusion equations. *Mathematics of Computation*, 82(283):1433–1462, 2013.
- C. Domingo-Enrich, J. Han, B. Amos, J. Bruna, and R. T. Q. Chen. Stochastic optimal control matching. *arXiv preprint arXiv:2312.02027*, 2023.
- C. Domingo-Enrich, M. Drozdal, B. Karrer, and R. T. Q. Chen. Adjoint matching: Fine-tuning flow and diffusion generative models with memoryless stochastic optimal control. *arXiv preprint arXiv:2409.08861*, 2024.
- W. E, J. Han, and A. Jentzen. Deep learning-based numerical methods for high-dimensional parabolic partial differential equations and backward stochastic differential equations. *Communications in Mathematics and Statistics*, 5(4):349–380, 2017.
- J. Feng and T. G. Kurtz. *Large deviations for stochastic processes*. Number 131. American Mathematical Soc., 2006.
- W. H. Fleming and J. L. Stein. Stochastic optimal control, international finance and debt. *Journal of Banking & Finance*, 28(5):979–996, 2004.
- E. Gobet. *Monte-Carlo methods and stochastic processes: from linear to non-linear*. CRC Press, 2016.
- E. Gobet, J.-P. Lemor, X. Warin, et al. A regression-based Monte Carlo method to solve backward stochastic differential equations. *The Annals of Applied Probability*, 15(3):2172–2202, 2005.

- A. Gorodetsky, S. Karaman, and Y. Marzouk. High-dimensional stochastic optimal control using continuous tensor decompositions. *International Journal of Robotics Research*, 37(2-3), 3 2018.
- J. Han and W. E. Deep learning approximation for stochastic control problems. *arXiv preprint arXiv:1611.07422*, 2016.
- J. Han, A. Jentzen, and W. E. Solving high-dimensional partial differential equations using deep learning. *Proceedings of the National Academy of Sciences*, 115(34):8505–8510, 2018.
- C. Hartmann and C. Schütte. Efficient rare event simulation by optimal nonequilibrium forcing. *Journal of Statistical Mechanics: Theory and Experiment*, 2012(11):P11004, 2012.
- C. Hartmann, R. Banisch, M. Sarich, T. Badowski, and C. Schütte. Characterization of rare events in molecular dynamics. *Entropy*, 16(1):350–376, 2014.
- C. Hartmann, L. Richter, C. Schütte, and W. Zhang. Variational characterization of free energy: Theory and algorithms. *Entropy*, 19(11), 2017.
- C. Hartmann, O. Kebiri, L. Neureither, and L. Richter. Variational approach to rare event simulation using least-squares regression. *Chaos: An Interdisciplinary Journal of Nonlinear Science*, 29(6):063107, 2019.
- L. Holdijk, Y. Du, F. Hooft, P. Jaini, B. Ensing, and M. Welling. Stochastic optimal control for collective variable free sampling of molecular transition paths. In *Thirty-seventh Conference on Neural Information Processing Systems*, 2023.
- M. Jensen and I. Smears. On the convergence of finite element methods for hamilton–jacobi–bellman equations. *SIAM Journal on Numerical Analysis*, 51(1):137–162, 2013.
- H. J. Kappen. Path integrals and symmetry breaking for optimal control theory. *Journal of Statistical Mechanics: Theory and Experiment*, 2005(11), nov 2005.
- H. J. Kappen and H. C. Ruiz. Adaptive importance sampling for control and inference. *Journal of Statistical Physics*, 162(5):1244–1266, 2016.
- P. Kidger, J. Foster, X. Li, H. Oberhauser, and T. Lyons. Neural sdes as infinite-dimensional gans. In *International Conference on Machine Learning*, 2021.
- X. Li, T.-K. L. Wong, R. T. Chen, and D. Duvenaud. Scalable gradients for stochastic differential equations. In *International Conference on Artificial Intelligence and Statistics*, pages 3870–3882. PMLR, 2020.
- J. Ma and J. Ma. Finite difference methods for the hamilton-jacobi-bellman equations arising in regime switching utility maximization. *J. Sci. Comput.*, 85(3):55, 2020.
- S. K. Mitter. Filtering and stochastic control: A historical perspective. *IEEE Control Systems Magazine*, 16(3):67–76, 1996.
- S. Mohamed, M. Rosca, M. Figurnov, and A. Mnih. Monte carlo gradient estimation in machine learning. *Journal of Machine Learning Research*, 21(132):1–62, 2020.
- N. Nüsken and L. Richter. Solving high-dimensional Hamilton–Jacobi–Bellman pdes using neural networks: perspectives from the theory of controlled diffusions and measures on path space. *Partial differential equations and applications*, 2:1–48, 2021.

- L. Ouyang, J. Wu, X. Jiang, D. Almeida, C. Wainwright, P. Mishkin, C. Zhang, S. Agarwal, K. Slama, A. Ray, J. Schulman, J. Hilton, F. Kelton, L. Miller, M. Simens, A. Aspell, P. Welinder, P. F. Christiano, J. Leike, and R. Lowe. Training language models to follow instructions with human feedback. In *Advances in Neural Information Processing Systems*, volume 35, pages 27730–27744. Curran Associates, Inc., 2022.
- H. Pham. *Continuous-time stochastic control and optimization with financial applications*, volume 61. Springer Science & Business Media, 2009.
- L. Pontryagin. *The Mathematical Theory of Optimal Processes*. Interscience Publishers, 1962.
- W. B. Powell and S. Meisel. Tutorial on stochastic optimization in energy—part i: Modeling and policies. *IEEE Transactions on Power Systems*, 31(2):1459–1467, 2016.
- S. Reich. Data assimilation: The Schrödinger perspective. *Acta Numerica*, 28:635–711, 2019.
- G. Roeder, Y. Wu, and D. K. Duvenaud. Sticking the landing: Simple, lower-variance gradient estimators for variational inference. In *Advances in Neural Information Processing Systems*, volume 30. Curran Associates, Inc., 2017.
- R. Y. Rubinstein and D. P. Kroese. *The cross-entropy method: a unified approach to combinatorial optimization, Monte-Carlo simulation and machine learning*. Springer Science & Business Media, 2013.
- J. Schulman, F. Wolski, P. Dhariwal, A. Radford, and O. Klimov. Proximal policy optimization algorithms. *arXiv preprint arXiv:1707.06347*, 2017.
- N. Stiennon, L. Ouyang, J. Wu, D. Ziegler, R. Lowe, C. Voss, A. Radford, D. Amodei, and P. F. Christiano. Learning to summarize with human feedback. In *Advances in Neural Information Processing Systems*, volume 33, pages 3008–3021. Curran Associates, Inc., 2020.
- H. J. Suh, M. Simchowitz, K. Zhang, and R. Tedrake. Do differentiable simulators give better policy gradients? In *International Conference on Machine Learning*, pages 20668–20696. PMLR, 2022.
- E. Theodorou, F. Stulp, J. Buchli, and S. Schaal. An iterative path integral stochastic optimal control approach for learning robotic tasks. *IFAC Proceedings Volumes*, 44(1):11594–11601, 2011. 18th IFAC World Congress.
- M. Uehara, Y. Zhao, K. Black, E. Hajiramezani, G. Scalia, N. L. Diamant, A. M. Tseng, T. Biancalani, and S. Levine. Fine-tuning of continuous-time diffusion models as entropy-regularized control. *arXiv preprint arXiv:2402.15194*, 2024.
- C. Villani. *Topics in Optimal Transportation*. Graduate studies in mathematics. American Mathematical Society, 2003.
- C. Villani. *Optimal Transport: Old and New*. Grundlehren der mathematischen Wissenschaften. Springer Berlin Heidelberg, 2008.
- J. Xu, X. Liu, Y. Wu, Y. Tong, Q. Li, M. Ding, J. Tang, and Y. Dong. Imagereward: Learning and evaluating human preferences for text-to-image generation. In *Thirty-seventh Conference on Neural Information Processing Systems*, 2023.
- J. Zhang et al. A numerical scheme for BSDEs. *The annals of applied probability*, 14(1):459–488, 2004.

- W. Zhang, H. Wang, C. Hartmann, M. Weber, and C. Schütte. Applications of the cross-entropy method to importance sampling and optimal control of diffusions. *SIAM Journal on Scientific Computing*, 36(6):A2654–A2672, 2014.
- M. Zhou, J. Han, and J. Lu. Actor-critic method for high dimensional static Hamilton–Jacobi–Bellman partial differential equations based on neural networks. *SIAM Journal on Scientific Computing*, 43(6):A4043–A4066, 2021.
- D. M. Ziegler, N. Stiennon, J. Wu, T. B. Brown, A. Radford, D. Amodei, P. Christiano, and G. Irving. Fine-tuning language models from human preferences. *arXiv preprint arXiv:1909.08593*, 2020.

# Contents

<b>A Preliminaries</b>	<b>17</b>
<b>B Sticking the Landing trick</b>	<b>19</b>
B.1 Sticking the Landing trick for the Continuous Adjoint loss . . . . .	20
B.2 Sticking the Landing trick for Adjoint Matching loss . . . . .	20
<b>C Derivation of the REINFORCE loss</b>	<b>20</b>
<b>D Theoretical guarantees of new SOC loss functions</b>	<b>22</b>
D.1 Proof of <b>Prop. 1</b> : theoretical guarantees of the Work-SOCM loss . . . . .	22
D.2 Proof of <b>Prop. 2</b> : theoretical guarantees of the Cost-SOCM loss . . . . .	23
D.3 Proof of <b>Prop. 3</b> : theoretical guarantees of the UW-SOCM loss . . . . .	24
<b>E Proofs of the taxonomy of SOC loss functions</b>	<b>25</b>
E.1 REINFORCE $\iff$ Discrete Adjoint . . . . .	25
E.2 REINFORCE $\iff$ REINFORCE (future rewards) . . . . .	25
E.3 Discrete Adjoint $\iff$ Continuous Adjoint . . . . .	26
E.4 Continuous Adjoint $\iff$ Cost-SOCM . . . . .	26
E.5 Bonus: REINFORCE (future rewards) $\iff$ Cost-SOCM . . . . .	26
E.6 Adjoint Matching $\iff$ Work-SOCM . . . . .	27
E.7 SOCM $\iff$ Cross Entropy . . . . .	28
E.8 SOCM $\iff$ SOCM-Adjoint . . . . .	28
E.9 Log-variance $\iff$ Moment . . . . .	29
<b>F Experimental details</b>	<b>29</b>
<b>G Additional experiments on simple SOC settings</b>	<b>29</b>

## A Preliminaries

**Theorem 2** (Girsanov theorem). *Let  $\mathbf{W} = (W_t)_{t \in [0, T]}$  be a standard Wiener process, and let  $\mathbb{P}$  be its induced probability measure over  $C([0, T]; \mathbb{R}^d)$ , known as the Wiener measure. Let  $(\Omega, \mathcal{F})$  be the  $\sigma$ -algebra associated to  $B_T$ . Let  $\theta_s$  be a locally- $\mathcal{H}_2$  process which is adapted to the natural filtration of the Brownian motion  $(B_t)_{t \geq 0}$ . For any  $F \in \mathcal{F}$ , define the measure*

$$\mathbb{Q}(F) = \mathbb{E}_{\mathbb{P}}[\exp(\int_0^T \theta_t dB_t - \frac{1}{2} \int_0^T \|\theta_t\|^2 dt) \mathbf{1}_F] .$$

$\mathbb{Q}$  is a probability measure. Under  $\mathbb{Q}$ , the stochastic process  $\{\tilde{W}(t)\}_{0 \leq t \leq T}$  defined as

$$\tilde{W}(t) = W(t) - \int_0^t \theta_s ds$$

is a standard Wiener process.

**Corollary 1** (Girsanov theorem for SDEs). *If the two SDEs*

$$\begin{aligned} dX_t &= b_1(X_t, t) dt + \sigma(X_t, t) dB_t, & X_0 &= x_{\text{init}} \\ dY_t &= (b_1(Y_t, t) + b_2(Y_t, t)) dt + \sigma(Y_t, t) dB_t, & Y_0 &= x_{\text{init}} \end{aligned}$$

admit unique strong solutions on  $[0, T]$ , then for any bounded continuous functional  $\Phi$  on  $C([0, T])$ , we have that

$$\begin{aligned}\mathbb{E}[\Phi(\mathbf{X})] &= \mathbb{E}\left[\Phi(\mathbf{Y}) \exp\left(-\int_0^T \sigma(Y_t, t)^{-1} b_2(Y_t, t) dB_t - \frac{1}{2} \int_0^T \|\sigma(Y_t, t)^{-1} b_2(Y_t, t)\|^2 dt\right)\right] \\ &= \mathbb{E}\left[\Phi(\mathbf{Y}) \exp\left(-\int_0^T \sigma(Y_t, t)^{-1} b_2(Y_t, t) d\tilde{B}_t + \frac{1}{2} \int_0^T \|\sigma(Y_t, t)^{-1} b_2(Y_t, t)\|^2 dt\right)\right],\end{aligned}$$

where  $\tilde{B}_t = B_t + \int_0^t \sigma(Y_s, s)^{-1} b_2(Y_s, s) ds$ . More generally,  $b_1$  and  $b_2$  can be random processes that are adapted to filtration of  $\mathbf{B}$ .

**Theorem 3** (Hamilton-Jacobi-Bellman equation). *If we define the infinitesimal generator*

$$\mathcal{L} := \frac{1}{2} \sum_{i,j=1}^d (\sigma \sigma^\top)_{ij}(t) \partial_{x_i} \partial_{x_j} + \sum_{i=1}^d b_i(x, t) \partial_{x_i},$$

the value function  $V$  for the SOC problem (1)-(2) solves the following Hamilton-Jacobi-Bellman (HJB) partial differential equation:

$$\begin{aligned}\partial_t V(x, t) &= -\mathcal{L}V(x, t) + \frac{1}{2} \|(\sigma^\top \nabla V)(x, t)\|^2 - f(x, t), \\ V(x, T) &= g(x).\end{aligned}$$

**Theorem 4** (Path-wise reparameterization trick, [Domingo-Enrich et al. \[2023\]](#), Prop. C.3). *Let  $(\Omega, \mathcal{F}, \mathbb{P})$  be a probability space, and  $\mathbf{B} : \Omega \times [0, T] \rightarrow \mathbb{R}^d$  be a Brownian motion. Let  $X : \Omega \times [0, T] \rightarrow \mathbb{R}^d$  be a process that satisfies the SDE  $dX_t = b(X_t, t) dt + \sigma(t) dB_t$ , and let  $\psi : \Omega \times \mathbb{R}^d \times [0, T] \rightarrow \mathbb{R}^d$  be an arbitrary random process such that:*

- For all  $z \in \mathbb{R}^d$ , the process  $\psi(\cdot, z, \cdot) : \Omega \times [0, T] \rightarrow \mathbb{R}^d$  is adapted to the filtration  $(\mathcal{F}_s)_{s \in [0, T]}$  of the Brownian motion  $\mathbf{B}$ .
- For all  $\omega \in \Omega$ ,  $\psi(\omega, \cdot, \cdot) : \mathbb{R}^d \times [0, T] \rightarrow \mathbb{R}^d$  is a twice-continuously differentiable function such that  $\psi(\omega, z, 0) = z$  for all  $z \in \mathbb{R}^d$ , and  $\psi(\omega, 0, s) = 0$  for all  $s \in [0, T]$ .

Let  $F : C([0, T]; \mathbb{R}^d) \rightarrow \mathbb{R}$  be a Fréchet-differentiable functional. We use the notation  $\mathbf{X} + \psi(z, \cdot) = (X_s(\omega) + \psi(\omega, z, s))_{s \in [0, T]}$  to denote the shifted process, but omit the dependency of  $\psi$  on  $\omega$ . Then,

$$\begin{aligned}\nabla_x \mathbb{E}[\exp(-F(\mathbf{X})) | X_0 = x] \\ = \mathbb{E}\left[\left(-\nabla_z F(\mathbf{X} + \psi(z, \cdot))\right)|_{z=0} + \int_0^T (\nabla_z \psi(0, s) \nabla_x b(X_s, s) - \nabla_z \partial_s \psi(0, s)) (\sigma^{-1})^\top(s) dB_s\right] \\ \times \exp(-F(\mathbf{X})) | X_0 = x].\end{aligned}$$

**Corollary 2** (Path-wise reparameterization trick for stochastic optimal control, [Domingo-Enrich et al. \[2023\]](#), Prop. 1). *For each  $t \in [0, T]$ , let  $M_t : [t, T] \rightarrow \mathbb{R}^{d \times d}$  be an arbitrary continuously differentiable function matrix-valued function such that  $M_t(t) = \text{Id}$ . We have that*

$$\begin{aligned}\nabla_x \mathbb{E}[\exp(-\int_t^T f(X_s, s) ds - g(X_T)) | X_t = x] \\ = \mathbb{E}\left[\left(-\int_t^T M_t(s) \nabla_x f(X_s, s) ds - M_t(T) \nabla g(X_T)\right) \right. \\ \left. + \int_t^T (M_t(s) \nabla_x b(X_s, s) - \partial_s M_t(s)) (\sigma^{-1})^\top(s) dB_s\right] \\ \times \exp(-\int_t^T f(X_s, s) ds - g(X_T)) | X_t = x].\end{aligned}$$

**Theorem 5** (Adjoint method for SDEs, Lemma 8 of [Domingo-Enrich et al. \[2023\]](#), [Li et al. \[2020\]](#), [Kidger et al. \[2021\]](#)). *Let  $\mathbf{X} : \Omega \times [0, T] \rightarrow \mathbb{R}^d$  be a stochastic process that satisfies the*

SDE  $dX_t = b(X_t, t) dt + \sigma(t) dB_t$ , with initial condition  $X_0 = x$ . We define the random process  $a : \Omega \times [0, T] \rightarrow \mathbb{R}^d$  such that for all  $\omega \in \Omega$ , using the short-hand  $a(t) := a(\omega, t)$ ,

$$\begin{aligned} da_t(\omega) &= (-\nabla_x b(X_t(\omega), t)a_t(\omega) - \nabla_x f(X_t(\omega), t)) dt - \nabla_x h(X_t(\omega), t) dB_t, \\ a_T(\omega) &= \nabla_x g(X_T(\omega)), \end{aligned}$$

we have that

$$\begin{aligned} &\nabla_x \mathbb{E} \left[ \int_0^T f(X_t(\omega), t) dt + \int_0^T \langle h(X_t(\omega), t), dB_t \rangle + g(X_T(\omega)) | X_0(\omega) = x \right] = \mathbb{E}[a_0(\omega)], \\ &\nabla_x \mathbb{E} \left[ \exp \left( - \int_0^T f(X_t(\omega), t) dt - \int_0^T \langle h(X_t(\omega), t), dB_t \rangle - g(X_T(\omega)) \right) | X_0(\omega) = x \right] \\ &= -\mathbb{E} \left[ a_0(\omega) \exp \left( - \int_0^T f(X_t(\omega), t) dt - \int_0^T \langle h(X_t(\omega), t), dB_t \rangle - g(X_T(\omega)) \right) | X_0(\omega) = x \right]. \end{aligned}$$

## B Sticking the Landing trick

**Remark 1** (Sticking the Landing trick). *For any  $v \in \mathcal{U}$ , we have the following:*

$$\begin{aligned} J(v; x, t) &:= \mathbb{E} \left[ \int_t^T \left( \frac{1}{2} \|v(X_s^v, s)\|^2 + f(X_s^v, s) \right) ds + g(X_T^v) | X_t^v = x \right] \\ &= \mathbb{E} \left[ \int_t^T \left( \frac{1}{2} \|v(X_s^v, s)\|^2 + f(X_s^v, s) \right) ds + \int_t^T \langle v(X_s^v, s), dB_s \rangle + g(X_T^v) | X_t^v = x \right] \end{aligned}$$

And for the optimal control  $u^*$ , we have that

$$\int_t^T \left( \frac{1}{2} \|u^*(X_s^{u^*}, s)\|^2 + f(X_s^{u^*}, s) \right) ds + \int_t^T \langle u^*(X_s^{u^*}, s), dB_s \rangle + g(X_T^{u^*}) = J(u^*; x, t) = V(X_t^{u^*}, t) \quad (28)$$

Hence, the left-hand side of (28) is a zero-variance estimator of  $J(u^*; x, t)$ . For  $v$  close to  $u^*$ , one can argue that

$$\int_t^T \left( \frac{1}{2} \|v(X_s^v, s)\|^2 + f(X_s^v, s) \right) ds + \int_t^T \langle v(X_s^v, s), dB_s \rangle + g(X_T^v)$$

is a low-variance estimator of  $J(v; x, t)$ , and hence, it is convenient to use this expression to replace  $\int_t^T \left( \frac{1}{2} \|v(X_s^v, s)\|^2 + f(X_s^v, s) \right) ds + g(X_T^v)$ , whenever needed. This amounts to including an additional term  $\int_t^T \langle v(X_s^v, s), dB_s \rangle$ .

*Proof.* To prove (28), we can assume without loss of generality that  $t = 0$ . We use that (see e.g. [Domingo-Enrich et al., 2023, Lemma 4])

$$\begin{aligned} \forall v \in \mathcal{U}, \quad \frac{d\mathbb{P}^v}{d\mathbb{P}}(X) &= \exp \left( \int_0^T \langle v(X_t, t), dB_t \rangle - \frac{1}{2} \int_0^T \|v(X_t, t)\|^2 dt \right), \\ \frac{d\mathbb{P}^{u^*}}{d\mathbb{P}^{u^*}}(X^{u^*}) &= \exp \left( \left( -V(X_0^{u^*}, 0) + \int_0^T f(X_s^{u^*}, s) ds + g(X_T^{u^*}) \right) \right), \end{aligned}$$

which means that

$$\begin{aligned} 1 &= \frac{d\mathbb{P}^{u^*}}{d\mathbb{P}}(X^{u^*}) \frac{d\mathbb{P}}{d\mathbb{P}^{u^*}}(X^{u^*}) \\ &= \exp \left( \int_0^T \langle v(X_t^{u^*}, t), dB_t^{u^*} \rangle - \frac{1}{2} \int_0^T \|v(X_t^{u^*}, t)\|^2 dt \right. \\ &\quad \left. + \left( -V(X_0^{u^*}, 0) + \int_0^T f(X_s^{u^*}, s) ds + g(X_T^{u^*}) \right) \right) \quad (29) \\ &= \exp \left( \int_0^T \langle v(X_t^{u^*}, t), dB_t \rangle + \frac{1}{2} \int_0^T \|v(X_t^{u^*}, t)\|^2 dt \right. \\ &\quad \left. + \left( -V(X_0^{u^*}, 0) + \int_0^T f(X_s^{u^*}, s) ds + g(X_T^{u^*}) \right) \right) \end{aligned}$$

where we used that  $B_t^{u^*} = B_t + \int_0^t v(X_s^{u^*}, s) ds$  or equivalently,  $dB_t^{u^*} = dB_t + v(X_t^{u^*}, t) dt$ . Equation (28) can be deduced directly from (29).  $\square$

## B.1 Sticking the Landing trick for the Continuous Adjoint loss

To derive the STL version of the Continuous Adjoint loss, we need to modify slightly the argument from [Domingo-Enrich et al. 2024](#), Lem. 5. We need to replace  $\int_t^T (\frac{1}{2}\|v(X_s^u, s)\|^2 + f(X_s^u, s)) ds + g(X_T^u)$  by  $\int_t^T (\frac{1}{2}\|v(X_s^u, s)\|^2 + f(X_s^u, s)) ds + \int_t^T \langle v(X_s^u, s), dB_s \rangle + g(X_T^u)$  everywhere in the proof. We end up with the following expression for the STL adjoint ODE:

$$\begin{aligned} da(t; X^{\bar{u}}, \bar{u}) &= - \left[ (\nabla_x (b(X_t^{\bar{u}}, t) + \sigma(t)u(X_t^{\bar{u}}, t)))^\top a(t; X^{\bar{u}}, \bar{u}) + \nabla_x (f(X_t^{\bar{u}}, t) + \frac{1}{2}\|\bar{u}(X_t^{\bar{u}}, t)\|^2) \right] dt \\ &\quad - \nabla_x \bar{u}(X_t^{\bar{u}}, t) dB_t, \\ a(T, X^{\bar{u}}) &= \nabla g(X_T^{\bar{u}}). \end{aligned}$$

Since the STL estimator has zero variance at the optimal control, the STL adjoint state also has zero variance when  $\bar{u}$  is the optimal control.

## B.2 Sticking the Landing trick for Adjoint Matching loss

To derive the STL version of the Adjoint Matching loss, we apply the same argument as in [[Domingo-Enrich et al., 2024](#), Sec. E.3], but we start from the STL adjoint ODE instead. We obtain the following expression for the lean STL adjoint ODE:

$$\begin{aligned} d\tilde{a}(t; X^{\bar{u}}, \bar{u}) &= -(\nabla_x b(X_t^{\bar{u}}, t)\tilde{a}(t, X^{\bar{u}}) + \nabla_x f(X_t^{\bar{u}}, t)) dt - \nabla_x \bar{u}(X_t^{\bar{u}}, t) dB_t, \\ \tilde{a}(T; X^{\bar{u}}, \bar{u}) &= \nabla g(X_T^{\bar{u}}). \end{aligned}$$

## C Derivation of the REINFORCE loss

**Proposition 4** (Derivation of the REINFORCE loss (12)). *The loss  $\mathcal{L}_{\text{RF}}$  in (12) is the continuous-time continuous-space analog of the REINFORCE loss for maximum entropy reinforcement learning.*

*Proof.* A similar derivation can be found in [Borrell et al. \[2022\]](#). By the Girsanov theorem for SDEs ([Cor. 1](#)), we can rewrite the control objective (1) in terms of the uncontrolled process (that is the process controlled by  $u \equiv 0$ , which we denote simply by  $X$ ):

$$\begin{aligned} &\mathbb{E} \left[ \int_0^T (\frac{1}{2}\|u(X_t^u, t)\|^2 + f(X_t^u, t)) dt + g(X_T^u) \right] \\ &= \mathbb{E} \left[ \left( \int_0^T (\frac{1}{2}\|u(X_t, t)\|^2 + f(X_t, t)) dt + g(X_T) \right) \right. \\ &\quad \left. \times \exp \left( \int_0^T \langle u(X_t, t), dB_t \rangle - \frac{1}{2} \int_0^T \|u(X_t, t)\|^2 dt \right) \right]. \end{aligned} \tag{30}$$

That is, we performed a change of process between the following pair:

$$\begin{aligned} dX_t^u &= (b(X_t^u, t) + \sigma(t)u(X_t^u, t)) dt + \sigma(t)dB_t, & X_0^u &\sim p_0, \\ dX_t &= (b(X_t, t) + \sigma(t)u(X_t, t) - \sigma(t)u(X_t, t)) dt + \sigma(t)dB_t, & X_0 &\sim p_0, \end{aligned}$$

which means that the tilted Brownian motion for the change of process is defined as  $\tilde{B}_t = B_t - \int_0^t u(X_s, s) ds$ .

The REINFORCE gradient for classical MaxEnt RL reads

$$\nabla_\theta \mathbb{E}_{\tau \sim \pi_{\theta, p}} \left[ \sum_{k=0}^K r_k(s_k, a_k) - \text{KL}(\pi_\theta(\cdot; s_k, k) \parallel \pi_{\text{base}}(\cdot; s_k, k)) \right],$$

where  $\pi_\theta$  is a policy parameterized by  $\theta$ . Following the connection between SOC and maximum entropy RL [Domingo-Enrich et al., 2024, App. C], the continuous-time continuous-space analog of the entropy-regularized expected reward is the SOC objective. Thus, if we have a control  $u_\theta$  parameterized by  $\theta$ , the REINFORCE control is given by

$$\nabla_\theta \mathbb{E} \left[ \int_0^T \left( \frac{1}{2} \|u_\theta(X_t^{u_\theta}, t)\|^2 + f(X_t^{u_\theta}, t) \right) dt + g(X_T^{u_\theta}) \right].$$

We develop this making use of the change of process in (30), which makes the dependence on the control  $u_\theta$  explicit:

$$\begin{aligned} & \nabla_\theta \mathbb{E} \left[ \int_0^T \left( \frac{1}{2} \|u_\theta(X_t^{u_\theta}, t)\|^2 + f(X_t^{u_\theta}, t) \right) dt + g(X_T^{u_\theta}) \right] \\ & \stackrel{(i)}{=} \mathbb{E} \left[ \int_0^T \nabla_\theta u_\theta(X_t, t) u_\theta(X_t, t) dt \times \exp \left( \int_0^T \langle u_\theta(X_t, t), dB_t \rangle - \frac{1}{2} \int_0^T \|u_\theta(X_t, t)\|^2 dt \right) \right. \\ & \quad + \left( \int_0^T \left( \frac{1}{2} \|u_\theta(X_t, t)\|^2 + f(X_t, t) \right) dt + g(X_T) \right) \\ & \quad \times \left( \int_0^T \nabla_\theta u_\theta(X_t, t) dB_t - \int_0^T \nabla_\theta u_\theta(X_t, t) u_\theta(X_t, t) dt \right) \\ & \quad \times \exp \left( \int_0^T \langle u_\theta(X_t, t), dB_t \rangle - \frac{1}{2} \int_0^T \|u_\theta(X_t, t)\|^2 dt \right) \Big] \\ & \stackrel{(ii)}{=} \mathbb{E} \left[ \int_0^T \nabla_\theta u_\theta(X_t, t) u_\theta(X_t, t) dt \times \exp \left( \int_0^T \langle u_\theta(X_t, t), dB_t \rangle - \frac{1}{2} \int_0^T \|u_\theta(X_t, t)\|^2 dt \right) \right. \\ & \quad + \left( \int_0^T \left( \frac{1}{2} \|u_\theta(X_t, t)\|^2 + f(X_t, t) \right) dt + g(X_T) \right) \\ & \quad \times \left( \int_0^T \nabla_\theta u_\theta(X_t, t) \underbrace{(dB_t - u_\theta(X_t, t) dt)}_{d\tilde{B}_t} + u_\theta(X_t, t) dt \right) \\ & \quad - \int_0^T \nabla_\theta u_\theta(X_t, t) u_\theta(X_t, t) dt \Big] \\ & \quad \times \exp \left( \int_0^T \langle u_\theta(X_t, t), dB_t \rangle - \frac{1}{2} \int_0^T \|u_\theta(X_t, t)\|^2 dt \right) \Big] \\ & \stackrel{(iii)}{=} \mathbb{E} \left[ \int_0^T \nabla_\theta u_\theta(X_t^{u_\theta}, t) u_\theta(X_t^{u_\theta}, t) dt \right. \\ & \quad + \left( \int_0^T \left( \frac{1}{2} \|u_\theta(X_t^{u_\theta}, t)\|^2 + f(X_t^{u_\theta}, t) \right) dt + g(X_T^{u_\theta}) \right) \\ & \quad \times \left( \int_0^T \nabla_\theta u_\theta(X_t^{u_\theta}, t) (dB_t + u_\theta(X_t^{u_\theta}, t) dt) \right. \\ & \quad \left. \left. - \int_0^T \nabla_\theta u_\theta(X_t^{u_\theta}, t) u_\theta(X_t^{u_\theta}, t) dt \right) \right] \\ & \stackrel{(iv)}{=} \mathbb{E} \left[ \int_0^T \nabla_\theta u_\theta(X_t^{u_\theta}, t) u_\theta(X_t^{u_\theta}, t) dt \right. \\ & \quad \left. + \left( \int_0^T \left( \frac{1}{2} \|u_\theta(X_t^{u_\theta}, t)\|^2 + f(X_t^{u_\theta}, t) \right) dt + g(X_T^{u_\theta}) \right) \times \int_0^T \nabla_\theta u_\theta(X_t^{u_\theta}, t) dB_t \right] \end{aligned}$$

In this derivation,

- Equality (i) holds by taking the derivative of the right-hand side of (30) with respect to  $\theta$ .
- Equality (ii) holds by adding and subtracting  $u_\theta(X_t, t) dt$  to  $dB_t$ , in order to express the stochastic integral in terms of the tilted Brownian motion  $\tilde{B}_t$ .
- Equality (iii) holds by applying the Girsanov theorem in the opposite direction, with a change of process from  $X$  to  $X^{u_\theta}$ . In these case, we need to use the full version of the theorem (Thm. 2), which states that the tilted Brownian motion  $\tilde{B}_t$  is a standard Brownian motion when the expectation contains the importance weight  $\exp \left( \int_0^T \langle u_\theta(X_t, t), dB_t \rangle - \frac{1}{2} \int_0^T \|u_\theta(X_t, t)\|^2 dt \right)$ .
- Equality (iv) is a straight-forward simplification.

To conclude the proof, observe that

$$\begin{aligned}
& \mathbb{E} \left[ \int_0^T \nabla_{\theta} u_{\theta}(X_t^{u_{\theta}}, t) u_{\theta}(X_t^{u_{\theta}}, t) dt \right. \\
& \quad \left. + \left( \int_0^T \left( \frac{1}{2} \|u_{\theta}(X_t^{u_{\theta}}, t)\|^2 + f(X_t^{u_{\theta}}, t) \right) dt + g(X_T^{u_{\theta}}) \right) \times \int_0^T \nabla_{\theta} u_{\theta}(X_t^{u_{\theta}}, t) dB_t \right] \\
&= \nabla_{\theta} \mathbb{E} \left[ \frac{1}{2} \int_0^T \|u_{\theta}(X_t^v, t)\|^2 dt \right. \\
& \quad \left. + \left( \int_0^T \left( \frac{1}{2} \|v(X_t^v, t)\|^2 + f(X_t^v, t) \right) dt + g(X_T^v) \right) \times \int_0^T u_{\theta}(X_t^v, t) dB_t \right]_{v=\text{stopgrad}(u_{\theta})} \\
&= \nabla_{\theta} \mathbb{E}[\mathcal{L}_{\text{RF}}(u_{\theta})].
\end{aligned}$$

□

## D Theoretical guarantees of new SOC loss functions

### D.1 Proof of **Prop. 1**: theoretical guarantees of the Work-SOCM loss

To prove that the gradients of the losses  $\mathcal{L}_{\text{Adj-Match}}$  and  $\mathcal{L}_{\text{Work-SOCM}}$  are equal, we first state a characterization of the solution  $\tilde{a}(t, X^v)$  of the Adjoint Matching ODE (9)-(10). By **Thm. 5**, we have that

$$\tilde{a}(t, X^v) = \nabla_{X_t} \left( \int_t^T f(X_s, s) ds + g(X_T) \right) |_{X=X^v}. \quad (31)$$

Here,  $X$  is the uncontrolled process, satisfying  $dX_t = b(X_t, t) dt + \sigma(t) dB_t$ ,  $X_0 = x$ . Recall that  $\mathcal{W}(t, X) = \int_t^T f(X_s, s) ds + g(X_T)$  is known as the work function, which is why Adjoint Matching is an appropriate name for the resulting loss.

From (31), we deduce that

$$\begin{aligned}
\mathbb{E}[\tilde{a}(t, X^v) | X_t^v = x] &= \mathbb{E}[\nabla_{X_t} \left( \int_t^T f(X_s, s) ds + g(X_T) \right) |_{X=X^v} | X_t^v = x] \\
&= \mathbb{E}[\nabla_{X_t} \left( \int_t^T f(X_s, s) ds + g(X_T) \right) \frac{d\mathbb{P}^v}{d\mathbb{P}}(X) | X_t = x] \\
&= \nabla_x \mathbb{E}[\left( \int_t^T f(X_s, s) ds + g(X_T) \right) \text{stopgrad} \left( \frac{d\mathbb{P}^v}{d\mathbb{P}}(X) \right) | X_t = x]
\end{aligned} \quad (32)$$

where  $\frac{d\mathbb{P}^v}{d\mathbb{P}}(X) = \exp \left( \int_t^T \langle v(X_s, s), dB_s \rangle - \frac{1}{2} \int_t^T \|v(X_s, s)\|^2 ds \right)$  by Girsanov's theorem (**Cor. 1**).

Next, we apply the path-wise reparameterization trick (**Thm. 4**), taking the uncontrolled process  $X$  between times  $t$  and  $T$  and defining  $F$  such that

$$\begin{aligned}
\exp(-F(X)) &= \left( \int_t^T f(X_s, s) ds + g(X_T) \right) \text{stopgrad} \left( \frac{d\mathbb{P}^v}{d\mathbb{P}}(X) \right) \\
\iff F(X) &= -\log \left( \left( \int_t^T f(X_s, s) ds + g(X_T) \right) \text{stopgrad} \left( \frac{d\mathbb{P}^v}{d\mathbb{P}}(X) \right) \right)
\end{aligned}$$

This means that

$$\begin{aligned}
\nabla_z F(X + \psi(z, \cdot)) |_{z=0} &= -\frac{\partial_z \left( \int_t^T f(X_s, s) ds + g(X_T) \right) |_{z=0} \text{stopgrad} \left( \frac{d\mathbb{P}^v}{d\mathbb{P}}(X) \right)}{\left( \int_t^T f(X_s, s) ds + g(X_T) \right) \text{stopgrad} \left( \frac{d\mathbb{P}^v}{d\mathbb{P}}(X) \right)} \\
&= -\frac{\int_t^T \nabla_z \psi(0, s) \nabla_x f(X_s, s) ds + \nabla_z \psi(0, T) \nabla_x g(X_T)}{\int_t^T f(X_s, s) ds + g(X_T)}
\end{aligned}$$

We conclude that

$$\begin{aligned}
\nabla_x \mathbb{E}[\exp(-F(X)) | X_0 = x] &= \mathbb{E}[( -\nabla_z F(X + \psi(z, \cdot)) |_{z=0} \\
&\quad + \int_t^T (\nabla_z \psi(0, s) \nabla_x b(X_s, s) - \nabla_z \partial_s \psi(0, s)) (\sigma^{-1})^\top(s) dB_s) \\
&\quad \times \exp(-F(X)) | X_t = x] \\
&= \mathbb{E}[( \int_t^T \nabla_z \psi(0, s) \nabla_x f(X_s, s) ds + \nabla_z \psi(0, T) \nabla_x g(X_T) \\
&\quad + \int_t^T (\nabla_z \psi(0, s) \nabla_x b(X_s, s) - \nabla_z \partial_s \psi(0, s)) (\sigma^{-1})^\top(s) dB_s \\
&\quad \times (\int_t^T f(X_s, s) ds + g(X_T))] \times \text{stopgrad}(\frac{d\mathbb{P}^v}{d\mathbb{P}}(X)) | X_t = x] \\
&= \mathbb{E}[\int_t^T \nabla_z \psi(0, s) \nabla_x f(X_s^v, s) ds + \nabla_z \psi(0, T) \nabla_x g(X_T^v) \\
&\quad + \int_t^T (\nabla_z \psi(0, s) \nabla_x b(X_s^v, s) - \nabla_z \partial_s \psi(0, s)) (\sigma^{-1})^\top(s) dB_s \\
&\quad \times (\int_t^T f(X_s^v, s) ds + g(X_T^v)) | X_t^v = x]
\end{aligned} \tag{33}$$

If we choose the perturbation  $\psi(z, s) = M_t(s)^\top z$  with  $M_t(t) = \text{Id}$ , we have that the conditions in [Thm. 4](#) are satisfied, and we have that  $\nabla \psi(z, s) = M_t(s)$ . Using this, and putting together [\(32\)](#) and [\(33\)](#), we obtain that

$$\begin{aligned}
\mathbb{E}[\tilde{a}(t, X^v) | X_t^v = x] &= \mathbb{E}[\int_t^T M_t(s) \nabla_x f(X_s^v, s) ds + M_t(T) \nabla_x g(X_T^v) \\
&\quad + \int_t^T (M_t(s) \nabla_x b(X_s^v, s) - \nabla_z M_t(s)) (\sigma^{-1})^\top(s) dB_s \\
&\quad \times (\int_t^T f(X_s^v, s) ds + g(X_T^v)) | X_t^v = x] \\
&= \mathbb{E}[\tilde{\xi}(t, v, X^v, B, M_t) | X_t^v = x].
\end{aligned} \tag{34}$$

Now, we can write a decomposition of the expected loss  $\mathbb{E}[\mathcal{L}_{\text{Work-SOCM}}]$  by adding and subtracting the conditional expectation of  $\sigma(t)^\top \tilde{\xi}(t, v, X^v, B, M_t)$ , which allows us to use [\(34\)](#):

$$\begin{aligned}
\mathbb{E}[\mathcal{L}_{\text{Work-SOCM}}(u)] &:= \mathbb{E}[\int_0^T \|u(X_t^v, t) + \sigma(t)^\top \mathbb{E}[\tilde{\xi}(t, v, X^v, B, M_t) | X_t^v]\|^2 dt] |_{v=\text{stopgrad}(u)} \\
&\quad + \mathbb{E}[\int_0^T \|\sigma(t)^\top (\mathbb{E}[\tilde{\xi}(t, v, X^v, B, M_t) | X_t^v] - \tilde{\xi}(t, v, X^v, B, M_t))\|^2 dt] |_{v=\text{stopgrad}(u)} \\
&= \mathbb{E}[\int_0^T \|u(X_t^v, t) + \sigma(t)^\top \mathbb{E}[\tilde{a}(t, X^v) | X_t^v = x]\|^2 dt] |_{v=\text{stopgrad}(u)} \\
&\quad + \mathbb{E}[\int_0^T \|\sigma(t)^\top (\mathbb{E}[\tilde{\xi}(t, v, X^v, B, M_t) | X_t^v] - \tilde{\xi}(t, v, X^v, B, M_t))\|^2 dt] |_{v=\text{stopgrad}(u)} \\
&= \mathbb{E}[\mathcal{L}_{\text{Adj-M}}(u)] - \mathbb{E}[\int_0^T \|\sigma(t)^\top (\mathbb{E}[\tilde{a}(t, X^v) | X_t^v] - \tilde{a}(t, X^v))\|^2 dt] |_{v=\text{stopgrad}(u)} \\
&\quad + \mathbb{E}[\int_0^T \|\sigma(t)^\top (\mathbb{E}[\tilde{\xi}(t, v, X^v, B, M_t) | X_t^v] - \tilde{\xi}(t, v, X^v, B, M_t))\|^2 dt] |_{v=\text{stopgrad}(u)}.
\end{aligned} \tag{35}$$

## D.2 Proof of [Prop. 2](#): theoretical guarantees of the Cost-SOCM loss

We rely on the path-wise reparameterization trick ([Thm. 4](#)), taking the process to be the process  $X^v$  controlled by  $v$  between times  $t$  and  $T$ , and

$$\begin{aligned}
\exp(-F(X^v)) &= \int_t^T (\frac{1}{2} \|v(X_s^v, s)\|^2 + f(X_s^v, s)) ds + g(X_T^v) + \int_t^T \langle v(X_s^v, s), dB_s \rangle \\
\iff F(X^v) &= -\log(\int_t^T (\frac{1}{2} \|v(X_s^v, s)\|^2 + f(X_s^v, s)) ds + g(X_T^v) + \int_t^T \langle v(X_s^v, s), dB_s \rangle)
\end{aligned}$$

This means that

$$\begin{aligned}\nabla_z F(X^v + \psi(z, \cdot))|_{z=0} &= -\frac{\partial_z \left( \int_t^T (\frac{1}{2} \|v(X_s^v + \psi(z, s), s)\|^2 + f(X_s^v + \psi(z, s), s)) ds + g(X_T^v + \psi(z, T)) + \int_t^T \langle v(X_s^v, s), dB_s \rangle \right)|_{z=0}}{\int_0^T (\frac{1}{2} \|v(X_s^v, s)\|^2 + f(X_s^v, s)) dt + g(X_T^v) + \int_t^T \langle v(X_s^v, s), dB_s \rangle} \\ &= -\frac{\int_t^T \nabla_z \psi(0, s) \nabla_x (\frac{1}{2} \|v(X_s^v, s)\|^2 + f(X_s^v, s)) ds + \nabla_z \psi(0, T) \nabla_x g(X_T^v) + \int_t^T \nabla_z \psi(0, s) \nabla_x v(X_s^v, s) dB_s}{\int_t^T (\frac{1}{2} \|v(X_s^v, s)\|^2 + f(X_s^v, s)) ds + g(X_T^v) + \int_t^T \langle v(X_s^v, s), dB_s \rangle}\end{aligned}$$

Let  $J(v; x, t) = \mathbb{E}[\int_t^T (\frac{1}{2} \|v(X_s^v, s)\|^2 + f(X_s^v, s)) ds + g(X_T^v) | X_t^v = x]$  be the cost functional. We conclude that

$$\begin{aligned}\nabla_x J(v; x, t) &= \nabla_x \mathbb{E}[\exp(-F(X^v)) | X_0 = x] \\ &= \mathbb{E}[\left(-\nabla_z F(X^v + \psi(z, \cdot))|_{z=0}\right. \\ &\quad \left.+ \int_t^T (\nabla_z \psi(0, s) \nabla_x (b(X_s^v, s) + \sigma(s)v(X_s^v, s)) - \nabla_z \partial_s \psi(0, s)) (\sigma^{-1})^\top(s) dB_s\right) \\ &\quad \left. \times \exp(-F(X^v)) | X_t^v = x\right] \\ &= \mathbb{E}[\int_t^T \nabla_z \psi(0, s) \nabla_x (\frac{1}{2} \|v(X_s^v, s)\|^2 + f(X_s^v, s)) ds + \nabla_z \psi(0, T) \nabla_x g(X_T^v) + \int_t^T \nabla_z \psi(0, s) \nabla_x v(X_s^v, s) dB_s \\ &\quad + \int_t^T (\nabla_z \psi(0, s) \nabla_x (b(X_s^v, s) + \sigma(s)v(X_s^v, s)) - \nabla_z \partial_s \psi(0, s)) (\sigma^{-1})^\top(s) dB_s \\ &\quad \times \left(\int_t^T (\frac{1}{2} \|v(X_s^v, s)\|^2 + f(X_s^v, s)) ds + g(X_T^v) + \int_t^T \langle v(X_s^v, s), dB_s \rangle\right) | X_t^v = x]\end{aligned}$$

If we choose the perturbation  $\psi(z, s) = M_t(s)^\top z$  with  $M_t(t) = \text{Id}$ , we have that the conditions in [Thm. 4](#) are satisfied, and we have that  $\nabla \psi(z, s) = M_t(s)$ . Thus,

$$\begin{aligned}\nabla_x J(v; x, t) &= \mathbb{E}[\int_t^T M_t(s) \nabla_x (\frac{1}{2} \|v(X_s^v, s)\|^2 + f(X_s^v, s)) ds + M_t(T) \nabla_x g(X_T^v) + \int_t^T \nabla_z \psi(0, s) \nabla_x v(X_s^v, s) dB_s \\ &\quad + \int_t^T (M_t(s) \nabla_x (b(X_s^v, s) + \sigma(s)v(X_s^v, s)) - \nabla_z M_t(s)) (\sigma^{-1})^\top(s) dB_s \\ &\quad \times \left(\int_t^T (\frac{1}{2} \|v(X_s^v, s)\|^2 + f(X_s^v, s)) ds + g(X_T^v) + \int_t^T \langle v(X_s^v, s), dB_s \rangle\right) | X_t^v = x] \\ &= \mathbb{E}[\xi(t, v, X^v, B, M_t) | X_t^v = x].\end{aligned}$$

Let  $a(t; X^v, v)$  be the solution of the adjoint ODE [\(5\)-\(6\)](#). [[Domingo-Enrich et al., 2024](#), Lem. 5] shows that  $\mathbb{E}[a(t, X^v) | X_t^v = x] = \nabla_x J(v; x, t)$ , which means that  $\mathbb{E}[\xi(t, v, X^v, B, M_t) | X_t^v = x] = \mathbb{E}[a(t, X^v) | X_t^v = x]$ . Writing out the decomposition of the expected loss  $\mathbb{E}[\mathcal{L}_{\text{Cost-SOCM}}]$  analogous to [\(35\)](#) concludes the proof:

$$\begin{aligned}\mathbb{E}[\mathcal{L}_{\text{Cost-SOCM}}(u, M)] &= \mathbb{E}\left[\int_0^T \|u(X_t^v, t) + \sigma(t)^\top \mathbb{E}[\xi(t, v, X^v, B, M_t) | X_t^v]\|^2 dt\right]_{v=\text{stopgrad}(u)} \\ &\quad + \mathbb{E}\left[\int_0^T \|\sigma(t)^\top (\mathbb{E}[\xi(t, v, X^v, B, M_t) | X_t^v] - \xi(t, v, X^v, B, M_t))\|^2 dt\right]_{v=\text{stopgrad}(u)} \\ &= \mathbb{E}[\mathcal{L}_{\text{Cont-Adj}}(u, M)] - \mathbb{E}\left[\int_0^T \|\sigma(t)^\top (\mathbb{E}[a(t, X^v) | X_t^v] - a(t, X^v))\|^2 dt\right]_{v=\text{stopgrad}(u)} \\ &\quad + \mathbb{E}\left[\int_0^T \|\sigma(t)^\top (\mathbb{E}[\xi(t, v, X^v, B, M_t) | X_t^v] - \xi(t, v, X^v, B, M_t))\|^2 dt\right]_{v=\text{stopgrad}(u)}.\end{aligned}$$

### D.3 Proof of [Prop. 3](#): theoretical guarantees of the UW-SOCM loss

Recall that for any  $M$ , the unique minimizer of  $\mathcal{L}_{\text{SOCM}}(\cdot, M)$  is the optimal control  $u^*$ , c.f. [[Domingo-Enrich et al., 2023](#), proof sketch of Theorem 3.1]. We compute the first variation of the loss  $\mathcal{L}_{\text{SOCM}}$  with respect to  $u$ :

$$\frac{\delta}{\delta u} \mathbb{E}[\mathcal{L}_{\text{SOCM}}(u, M)](x, t) = \mathbb{E}[(u(X_t^v, t) + \sigma(t)^\top \omega(t, v, X^v, B, M_t)) \times \alpha(v, X^v, B) | X_t^v = x],$$

where  $v$  is arbitrary. This is because for any perturbation  $\tilde{u}$ , we have that

$$\begin{aligned} & \lim_{\epsilon \rightarrow 0} \mathbb{E} \left[ \int_0^T \left\| u(X_t^v, t) + \epsilon \tilde{u}(X_t^v, t) + \sigma(t)^\top \omega(t, v, X^v, B, M_t) \right\|^2 dt \times \alpha(v, X^v, B) \right] \\ &= \mathbb{E} \left[ \int_0^T \langle u(X_t^v, t) + \sigma(t)^\top \omega(t, v, X^v, B, M_t), \tilde{u}(X_t^v, t) \rangle dt \times \alpha(v, X^v, B) \right] \\ &= \int_0^T \mathbb{E} \left[ \langle \mathbb{E}[u(X_t^v, t) + \sigma(t)^\top \omega(t, v, X^v, B, M_t)] \times \alpha(v, X^v, B) | X_t^v \rangle, \tilde{u}(X_t^v, t) \rangle \right] dt \end{aligned}$$

Now, if we set  $v = u^*$ , we have that  $\alpha(u^*, X^{u^*}, B) = \exp(-V(X_0^{u^*}, 0))$ , and thus,

$$\begin{aligned} & \frac{\delta}{\delta u} \mathbb{E}[\mathcal{L}_{\text{SOCM}}(u, M)](x, t) \\ &= \mathbb{E}[(u(X_t^{u^*}, t) + \sigma(t)^\top \omega(t, u^*, X^{u^*}, B, M_t)) \times \exp(-V(X_0^{u^*}, 0)) | X_t^{u^*} = x] \\ &= \mathbb{E}[(u(X_t^{u^*}, t) + \sigma(t)^\top \omega(t, u^*, X^{u^*}, B, M_t)) | X_t^{u^*} = x] \times \mathbb{E}[\exp(-V(X_0^{u^*}, 0)) | X_t^{u^*} = x] \\ &= (u(x, t) + \sigma(t)^\top \mathbb{E}[\omega(t, u^*, X^{u^*}, B, M_t) | X_t^{u^*} = x]) \times \mathbb{E}[\exp(-V(X_0^{u^*}, 0)) | X_t^{u^*} = x]. \end{aligned}$$

Here, the second equality holds by the Markov property, which implies that  $X_{[t, T]}^{u^*}$  and  $X_0^{u^*}$  are conditionally independent given  $X_t^{u^*}$ . If we follow the same approach for  $\mathbb{E}[\mathcal{L}_{\text{UW-SOCM}}]$ , we obtain that

$$\begin{aligned} \frac{\delta}{\delta u} \mathbb{E}[\mathcal{L}_{\text{UW-SOCM}}(u, M)](x, t) &= \mathbb{E}[u(X_t^v, t) + \sigma(t)^\top \omega(t, v, X^v, B, M_t) | X_t^v = x] \Big|_{v=\text{stopgrad}(u)} \\ &= u(x, t) + \sigma(t)^\top \mathbb{E}[\omega(t, v, X^v, B, M_t) | X_t^v = x] \Big|_{v=\text{stopgrad}(u)}. \end{aligned}$$

Note that  $\frac{\delta}{\delta u} \mathbb{E}[\mathcal{L}_{\text{SOCM}}(u^*, M)](x, t)$  is everywhere zero because  $u^*$  is the unique optimizer of  $\mathbb{E}[\mathcal{L}_{\text{SOCM}}(\cdot, M)]$  for any  $M$ . Since the factor  $\mathbb{E}[\exp(-V(X_0^{u^*}, 0)) | X_t^{u^*} = x]$  is non-negative, the fact that the first variation  $\frac{\delta}{\delta u} \mathbb{E}[\mathcal{L}_{\text{SOCM}}(u^*, M)](x, t)$  is zero everywhere implies that  $\frac{\delta}{\delta u} \mathbb{E}[\mathcal{L}_{\text{UW-SOCM}}(u^*, M)](x, t)$  is zero everywhere as well. Hence,  $u^*$  is a critical point of  $\mathbb{E}[\mathcal{L}_{\text{UW-SOCM}}(\cdot, M)]$ .

## E Proofs of the taxonomy of SOC loss functions

We subdivide the proof of [Thm. 1](#) into showing that pairs of losses share the same gradient in expectation.

### E.1 REINFORCE $\iff$ Discrete Adjoint

As shown in the proof of [Prop. 4](#), we have that

$$\begin{aligned} \nabla_\theta \mathbb{E}[\mathcal{L}_{\text{RF}}(u_\theta)] &= \mathbb{E} \left[ \int_0^T \nabla_\theta u_\theta(X_t^{u_\theta}, t) u_\theta(X_t^{u_\theta}, t) dt \right. \\ &\quad \left. + \left( \int_0^T \left( \frac{1}{2} \|u_\theta(X_t^{u_\theta}, t)\|^2 + f(X_t^{u_\theta}, t) \right) dt + g(X_T^{u_\theta}) \right) \times \int_0^T \nabla_\theta u_\theta(X_t^{u_\theta}, t) dB_t \right] \quad (36) \\ &= \nabla_\theta \mathbb{E} \left[ \int_0^T \left( \frac{1}{2} \|u_\theta(X_t^{u_\theta}, t)\|^2 + f(X_t^{u_\theta}, t) \right) dt + g(X_T^{u_\theta}) \right] \end{aligned}$$

and the right-hand side is by definition equal to  $\nabla_\theta \mathbb{E}[\mathcal{L}_{\text{Disc-Adj}}(u_\theta)]$ .

### E.2 REINFORCE $\iff$ REINFORCE (future rewards)

This statement is the analog of a well-known fact in classical RL. By the definition of  $\mathcal{L}_{\text{RFFR}}$  in [\(13\)](#), we have that

$$\begin{aligned} \nabla_\theta \mathbb{E}[\mathcal{L}_{\text{RFFR}}(u_\theta)] &= \mathbb{E} \left[ \int_0^T \nabla_\theta u_\theta(X_t^{u_\theta}, t) u_\theta(X_t^{u_\theta}, t) dt \right. \\ &\quad \left. + \int_0^T \nabla_\theta u_\theta(X_t^{u_\theta}, t) \left( \int_t^T \left( \frac{1}{2} \|u_\theta(X_s^{u_\theta}, s)\|^2 + f(X_s^{u_\theta}, s) \right) ds + g(X_T^{u_\theta}) \right) dB_t \right]. \quad (37) \end{aligned}$$

Comparing (36) with (37), it suffices to check that

$$\begin{aligned} & \mathbb{E} \left[ \int_0^T \nabla_{\theta} u_{\theta}(X_t^{u_{\theta}}, t) \left( \int_0^T \left( \frac{1}{2} \|u_{\theta}(X_s^{u_{\theta}}, s)\|^2 + f(X_s^{u_{\theta}}, s) \right) ds + g(X_T^{u_{\theta}}) \right) dB_t \right] \\ &= \mathbb{E} \left[ \int_0^T \nabla_{\theta} u_{\theta}(X_t^{u_{\theta}}, t) \left( \int_t^T \left( \frac{1}{2} \|u_{\theta}(X_s^{u_{\theta}}, s)\|^2 + f(X_s^{u_{\theta}}, s) \right) ds + g(X_T^{u_{\theta}}) \right) dB_t \right] \end{aligned}$$

Or equivalently, it is enough to check that

$$\begin{aligned} 0 &= \mathbb{E} \left[ \int_0^T \nabla_{\theta} u_{\theta}(X_t^{u_{\theta}}, t) \int_0^t \left( \frac{1}{2} \|u_{\theta}(X_s^{u_{\theta}}, s)\|^2 + f(X_s^{u_{\theta}}, s) \right) ds dB_t \right] \\ &= \mathbb{E} \left[ \int_0^T \int_s^T \nabla_{\theta} u_{\theta}(X_t^{u_{\theta}}, t) dB_t \left( \frac{1}{2} \|u_{\theta}(X_s^{u_{\theta}}, s)\|^2 + f(X_s^{u_{\theta}}, s) \right) ds \right], \end{aligned} \quad (38)$$

where in the second equality we flipped the order of the deterministic and the stochastic integral using Fubini's theorem. Now, using the tower of expectations property, we can reexpress the right-hand side of (38) as

$$\mathbb{E} \left[ \int_0^T \mathbb{E} \left[ \int_s^T \nabla_{\theta} u_{\theta}(X_t^{u_{\theta}}, t) dB_t | X_s^{u_{\theta}} \right] \left( \frac{1}{2} \|u_{\theta}(X_s^{u_{\theta}}, s)\|^2 + f(X_s^{u_{\theta}}, s) \right) ds \right] = 0.$$

This is zero because Ito stochastic integrals are martingales.

### E.3 Discrete Adjoint $\iff$ Continuous Adjoint

This is shown in [Domingo-Enrich et al. 2024](#), Sec. E.1.

### E.4 Continuous Adjoint $\iff$ Cost-SOCM

This is shown in [Prop. 2](#).

### E.5 Bonus: REINFORCE (future rewards) $\iff$ Cost-SOCM

By transitivity, we have already shown that REINFORCE (future rewards) and Cost-SOCM have the same gradients in expectation, because we have shown equality between (i) REINFORCE (future rewards) and REINFORCE, (ii) REINFORCE and Discrete Adjoint, (iii) Discrete Adjoint and Continuous Adjoint, (iv) Continuous Adjoint and Cost-SOCM. Still, there is a direct way to show the equivalence between these two losses which helps flesh out their relationship in a clearer way: REINFORCE (future rewards) is simply Cost-SOCM with a particular choice of matrix  $M$ . The proof follows.

We can write

$$\begin{aligned} & \nabla_{\theta} \mathbb{E}[\mathcal{L}_{\text{Cost-SOCM}}(u_{\theta})] \\ &= 2 \mathbb{E} \left[ \int_0^T \nabla_{\theta} u_{\theta}(X_t^{u_{\theta}}, t) u_{\theta}(X_t^{u_{\theta}}, t) dt \right. \\ & \quad + \int_0^T \nabla_{\theta} u_{\theta}(X_t^{u_{\theta}}, t) \sigma(t)^{\top} \left( \int_t^T M_t(s) \nabla_x (f(X_s^{u_{\theta}}, s) + \frac{1}{2} \|u_{\theta}(X_s^{u_{\theta}}, s)\|^2) ds + M_t(T) \nabla g(X_T^{u_{\theta}}) \right. \\ & \quad \left. \left. + \left( \int_t^T (f(X_s^{u_{\theta}}, s) + \frac{1}{2} \|u_{\theta}(X_s^{u_{\theta}}, s)\|^2) ds + g(X_T^{u_{\theta}}) \right) \right. \right. \\ & \quad \left. \left. \times \left( \int_t^T (M_t(s) \nabla_x (b(X_s^{u_{\theta}}, s) + \sigma(s) u_{\theta}(X_s^{u_{\theta}}, s)) - \partial_s M_t(s)) (\sigma^{-1})^{\top}(s) dB_s \right) \right) dt \right]. \end{aligned}$$

Since  $M$  is arbitrary under the conditions that it is continuous and differentiable almost everywhere, and  $M_t(t) = \text{Id}$ , we are free to set  $M$  of the form

$$M_t^{(h)}(s) = \begin{cases} \left(1 - \frac{s-t}{h(T-t)}\right) \text{Id} & \text{if } s \in [t, t + h(T-t)], \\ 0 & \text{otherwise,} \end{cases}$$

we have that

$$\begin{aligned} & \lim_{h \rightarrow 0} \int_t^T M_t^{(h)}(s) \nabla_x (f(X_s^{u_\theta}, s) + \frac{1}{2} \|u_\theta(X_s^{u_\theta}, s)\|^2) ds + M_t^{(h)}(T) \nabla g(X_T^{u_\theta}) \\ &= \lim_{h \rightarrow 0} \int_t^{t+h(T-t)} M_t^{(h)}(s) \nabla_x (f(X_s^{u_\theta}, s) + \frac{1}{2} \|u_\theta(X_s^{u_\theta}, s)\|^2) ds = 0, \end{aligned} \quad (39)$$

and similarly,

$$\begin{aligned} & \lim_{h \rightarrow 0} \int_t^T M_t(s) \nabla_x (b(X_s^{u_\theta}, s) + \sigma(s) u_\theta(X_s^{u_\theta}, s)) (\sigma^{-1})^\top(s) dB_s \\ &= \lim_{h \rightarrow 0} \int_t^{t+h(T-t)} M_t(s) \nabla_x (b(X_s^{u_\theta}, s) + \sigma(s) u_\theta(X_s^{u_\theta}, s)) (\sigma^{-1})^\top(s) dB_s = 0. \end{aligned} \quad (40)$$

Finally,

$$\begin{aligned} & \int_0^T \nabla_\theta u_\theta(X_t^{u_\theta}, t) \sigma(t)^\top \left( \int_t^T (f(X_s^{u_\theta}, s) + \frac{1}{2} \|u_\theta(X_s^{u_\theta}, s)\|^2) ds + g(X_T^{u_\theta}) \right) \\ & \quad \times \left( \int_t^T \partial_s M_t^{(h)}(s) (\sigma^{-1})^\top(s) dB_s \right) dt \\ &= - \int_0^T \nabla_\theta u_\theta(X_t^{u_\theta}, t) \sigma(t)^\top \left( \int_t^T (f(X_{s'}^{u_\theta}, s') + \frac{1}{2} \|u_\theta(X_{s'}^{u_\theta}, s')\|^2) ds' + g(X_T^{u_\theta}) \right) \\ & \quad \times \frac{1}{h(T-t)} \left( \int_t^{t+h(T-t)} (\sigma^{-1})^\top(s) dB_s \right) dt \\ &= - \int_0^T \int_t^{t+h(T-t)} \varphi(t) \frac{1}{h(T-t)} (\sigma^{-1})^\top(s) dB_s dt \\ &= - \int_0^{hT} \int_0^s \varphi(t) \frac{1}{h(T-t)} (\sigma^{-1})^\top(s) dB_s - \int_{hT}^T \int_{\frac{s-hT}{1-h}}^s \varphi(t) \frac{1}{h(T-t)} (\sigma^{-1})^\top(s) dB_s \end{aligned} \quad (41)$$

where we defined  $\varphi(t) = \nabla_\theta u_\theta(X_t^{u_\theta}, t) \sigma(t)^\top \left( \int_t^T (f(X_{s'}^{u_\theta}, s') + \frac{1}{2} \|u_\theta(X_{s'}^{u_\theta}, s')\|^2) ds' + g(X_T^{u_\theta}) \right)$  in the second equality, and we used Fubini's theorem in the third equality. Note that

$$\lim_{h \rightarrow 0} \int_0^{hT} \int_0^s \varphi(t) \frac{1}{h(T-t)} (\sigma^{-1})^\top(s) dB_s = 0, \quad (42)$$

and

$$\begin{aligned} & \lim_{h \rightarrow 0} \int_{hT}^T \int_{\frac{s-hT}{1-h}}^s \varphi(t) \frac{1}{h(T-t)} (\sigma^{-1})^\top(s) dB_s \\ &= \lim_{h \rightarrow 0} \int_0^T \left( s - \frac{s-hT}{1-h} \right) \varphi(s) \frac{1}{h(T-s)} (\sigma^{-1})^\top(s) dB_s \\ &= \lim_{h \rightarrow 0} \int_0^T \left( s - \frac{s-hT}{1-h} \right) \varphi(s) \frac{1}{h(T-s)} (\sigma^{-1})^\top(s) dB_s \\ &= \int_0^T \varphi(s) (\sigma^{-1})^\top(s) dB_s \\ &= \int_0^T \nabla_\theta u_\theta(X_s^{u_\theta}, s) \sigma(s)^\top \left( \int_s^T (f(X_{s'}^{u_\theta}, s') + \frac{1}{2} \|u_\theta(X_{s'}^{u_\theta}, s')\|^2) ds' + g(X_T^{u_\theta}) \right) (\sigma^{-1})^\top(s) dB_s \\ &= \int_0^T \nabla_\theta u_\theta(X_s^{u_\theta}, s) \left( \int_s^T (f(X_{s'}^{u_\theta}, s') + \frac{1}{2} \|u_\theta(X_{s'}^{u_\theta}, s')\|^2) ds' + g(X_T^{u_\theta}) \right) dB_s \end{aligned} \quad (43)$$

If we plug (42) and (43) into (41), and then (39), (40) and (41) into (37), we obtain that

$$\begin{aligned} & \nabla_\theta \mathbb{E}[\mathcal{L}_{\text{Cost-SOCM}}(u_\theta)] \\ &= 2 \mathbb{E} \left[ \int_0^T \nabla_\theta u_\theta(X_t^{u_\theta}, t) u_\theta(X_t^{u_\theta}, t) dt \right. \\ & \quad \left. + \int_0^T \nabla_\theta u_\theta(X_t^{u_\theta}, t) \left( \int_t^T (f(X_s^{u_\theta}, s) + \frac{1}{2} \|u_\theta(X_s^{u_\theta}, s)\|^2) ds + g(X_T^{u_\theta}) \right) dB_t \right] \\ &= 2 \nabla_\theta \mathbb{E}[\mathcal{L}_{\text{RFFR}}(u_\theta)], \end{aligned}$$

where the last equality concludes the proof and holds by the definition of  $\mathcal{L}_{\text{RFFR}}$  (see (37)).

## E.6 Adjoint Matching $\iff$ Work-SOCM

This is shown in [Prop. 1](#).

## E.7 SOCM $\iff$ Cross Entropy

This result was proven in [Domingo-Enrich et al. \[2023\]](#). Namely, [[Domingo-Enrich et al., 2023](#), Prop. B.6(ii)] shows that

$$\mathbb{E}[\mathcal{L}_{\text{CE}}(u)] = \frac{1}{2} \mathbb{E} \left[ \int_0^T \|u^*(X_t^{u^*}, t) - u(X_t^{u^*}, t)\|^2 dt \exp(-V(X_0^{u^*}, 0)) \right],$$

and [[Domingo-Enrich et al., 2023](#), Prop. 3.3] shows that

$$\mathbb{E}[\mathcal{L}_{\text{SOCM}}(u, M)] = \mathbb{E} \left[ \int_0^T \|u(X_t^{u^*}, t) - u^*(X_t^{u^*}, t)\|^2 dt \exp(-V(X_0^{u^*}, 0)) \right] + \text{CondVar}(-\sigma(t)^\top \omega; M),$$

where the second term does not depend on  $u$ :

$$\text{CondVar}(-\sigma(t)^\top \omega; M) := \mathbb{E} \left[ \int_0^T \left\| \sigma(t)^\top \left( \omega(t, v, X^v, B, M_t) - \frac{\mathbb{E}[\omega(t, v, X^v, B, M_t) \alpha(v, X^v, B) | X_t^v, t]}{\mathbb{E}[\alpha(v, X^v, B) | X_t^v, t]} \right) \right\|^2 dt \alpha(v, X^v, B) \right].$$

## E.8 SOCM $\iff$ SOCM-Adjoint

This is also shown by [Domingo-Enrich et al. \[2023\]](#), putting together different results in their work. We reproduce their argument. The proof sketch of their Theorem 3.1 considers the following loss (up to constant factors and constant terms):

$$\begin{aligned} \tilde{\mathcal{L}}(u) &= \mathbb{E} \left[ \int_0^T (\|u(X_t, t)\|^2 - 2\langle u(X_t, t), u^*(X_t, t) \rangle) dt \times \exp \left( - \int_0^T f(X_t, t) dt - g(X_T) \right) \right] \\ &= \mathbb{E} \left[ \int_0^T (\|u(X_t, t)\|^2 - 2\langle u(X_t, t), u^*(X_t, t) \rangle) dt \right. \\ &\quad \left. \times \exp \left( - \int_0^T f(X_t, t) dt - g(X_T) \right) \right]. \\ &= \mathbb{E} \left[ \int_0^T \|u(X_t, t)\|^2 \times \exp \left( - \int_0^T f(X_t, t) dt - g(X_T) \right) \right] \\ &\quad - 2 \mathbb{E} \left[ \int_0^T \langle u(X_t, t), \sigma(t)^\top \nabla_x \mathbb{E} \left[ \exp \left( - \int_t^T f(X_s, s) ds - g(X_T) \right) | X_t = x \right] \rangle dt \right. \\ &\quad \left. \times \exp \left( - \int_0^t f(X_s, s) ds \right) \right]. \end{aligned} \tag{44}$$

On the one-hand, the path-wise reparameterization ([Thm. 4](#), [[Domingo-Enrich et al., 2023](#), Prop. C.3]) trick yields

$$\begin{aligned} &\nabla_x \mathbb{E} \left[ \exp \left( - \int_t^T f(X_s, s) ds - g(X_T) \right) | X_t = x \right] \\ &= \mathbb{E} \left[ \left( - \int_t^T M_t(s) \nabla_x f(X_s, s) ds - M_t(T) \nabla g(X_T) \right. \right. \\ &\quad \left. \left. + \int_t^T (M_t(s) \nabla_x b(X_s, s) - \partial_s M_t(s)) (\sigma^{-1})^\top(s) dB_s \right) \right. \\ &\quad \left. \times \exp \left( - \int_t^T f(X_s, s) ds - g(X_T) \right) | X_t = x \right], \end{aligned}$$

and plugging this into the right-hand side of (44) yields the SOCM loss  $\mathcal{L}_{\text{SOCM}}$  after a change of process from  $X$  to  $X^v$ . On the other-hand, the same gradient can be estimated using the adjoint method ([Thm. 5](#), [[Domingo-Enrich et al., 2023](#), Lemma C.6]):

$$\begin{aligned} &\nabla_x \mathbb{E} \left[ \exp \left( - \int_t^T f(X_t, t) dt - g(X_T) \right) | X_t = x \right] \\ &= - \mathbb{E} \left[ a(t, X) \exp \left( - \int_0^T f(X_t, t) dt - g(X_T) \right) | X_t = x \right]. \end{aligned}$$

where  $a(t, X)$  is the solution of the lean adjoint ODE (9)-(10) (without the SLT term). Plugging this into the right-hand side of (44) yields the SOCM-Adjoint loss  $\mathcal{L}_{\text{SOCM-Adj}}$  after a change of process from  $X$  to  $X^v$ .

## E.9 Log-variance $\iff$ Moment

This is a simple observation that was first made by [Nüsken and Richter \[2021\]](#). When each batch contains  $m$  trajectories, the empirical log-variance loss reads

$$\mathcal{L}_{\text{Var}_v}^{\text{log},m}(u) := \frac{1}{m} \sum_{i=1}^m (\tilde{Y}_T^{u,v,(i)} - g(X_T^{v,(i)}))^2 - \left( \frac{1}{m} \sum_{i=1}^m (\tilde{Y}_T^{u,v,(i)} - g(X_T^{v,(i)})) \right)^2.$$

Thus,

$$\begin{aligned} \mathbb{E}[\mathcal{L}_{\text{Var}_v}^{\text{log},m}(u)] &= \mathbb{E}\left[\frac{1}{m} \sum_{i=1}^m (\tilde{Y}_T^{u,v,(i)} - g(X_T^{v,(i)}))^2\right] \\ &\quad - \mathbb{E}\left[\left(\frac{1}{m} \sum_{i=1}^m (\tilde{Y}_T^{u,v,(i)} - g(X_T^{v,(i)}))\right)^2\right] \\ &= \mathbb{E}[(\tilde{Y}_T^{u,v} - g(X_T^v))^2] - \mathbb{E}\left[\left(\frac{1}{m} \sum_{i=1}^m (\tilde{Y}_T^{u,v,(i)} - g(X_T^{v,(i)}))\right)^2\right]. \end{aligned}$$

Note that as  $m \rightarrow +\infty$ ,  $\mathbb{E}\left[\left(\frac{1}{m} \sum_{i=1}^m (\tilde{Y}_T^{u,v,(i)} - g(X_T^{v,(i)}))\right)^2\right] \rightarrow \mathbb{E}[\tilde{Y}_T^{u,v} - g(X_T^v)]^2$ , which means that

$$\lim_{m \rightarrow \infty} \mathcal{L}_{\text{Var}_v}^{\text{log},m}(u) = \mathbb{E}[(\tilde{Y}_T^{u,v} - g(X_T^v))^2] - \mathbb{E}[\tilde{Y}_T^{u,v} - g(X_T^v)]^2.$$

And for any  $u, v$ , we have that

$$\begin{aligned} \min_{y_0 \in \mathbb{R}} \mathcal{L}_{\text{Mom}_v}(u, y_0) &= \min_{y_0 \in \mathbb{R}} \mathbb{E}[(\tilde{Y}_T^{u,v} + y_0 - g(X_T^v))^2] \\ &= \mathbb{E}[(\tilde{Y}_T^{u,v} - g(X_T^v) - \mathbb{E}[\tilde{Y}_T^{u,v} - g(X_T^v)])^2] \\ &= \mathbb{E}[(\tilde{Y}_T^{u,v} - g(X_T^v))^2] - \mathbb{E}[\tilde{Y}_T^{u,v} - g(X_T^v)]^2, \end{aligned}$$

which shows that when  $y_0$  is optimized instantaneously, the two losses coincide.

## F Experimental details

We use the experimental setup of [Domingo-Enrich et al. \[2023\]](#), which was partially based on that of [Nüsken and Richter \[2021\]](#). We use the same hyperparameters and same architectures as [Domingo-Enrich et al. \[2023\]](#). We include an additional setting: DOUBLE WELL, HARD, which is given by

$$b(x, t) = -\nabla \Psi(x), \quad \Psi(x) = \sum_{i=1}^d \kappa_i (x_i^2 - 1)^2, \quad g(x) = \sum_{i=1}^d \nu_i (x_i^2 - 1)^2, \quad f(x) = 0, \quad \sigma_0 = \text{I},$$

where  $d = 10$ , and  $\kappa_i = 5$ ,  $\nu_i = 6$  for  $i \in \{1, 2, 3\}$  and  $\kappa_i = 1$ ,  $\nu_i = 2$  for  $i \in \{4, \dots, 10\}$ . We set  $T = 1$ ,  $\lambda = 1$  and  $x_{\text{init}} = 0$ . Our DOUBLE WELL, EASY setting corresponds to the DOUBLE WELL setting from [Domingo-Enrich et al. \[2023\]](#), and it corresponds to setting  $\kappa_i = 5$ ,  $\nu_i = 3$  for  $i \in \{1, 2, 3\}$  and  $\kappa_i = 1$ ,  $\nu_i = 1$  for  $i \in \{4, \dots, 10\}$ .

## G Additional experiments on simple SOC settings

[Figure 3](#) shows the control  $L^2$  error curves for Adjoint Matching, Continuous Adjoint and Discrete Adjoint, each with and without the Sticking the Landing (STL) trick. We make the following observations:

- The Discrete Adjoint loss with STL performs substantially worse than the the Discrete Adjoint loss without STL, while the Continuous Adjoint and Adjoint Matching losses with STL do better. The reason for this is that the Discrete Adjoint loss with STL directly optimizes the loss

$$\mathcal{L}(u; X^u) := \int_0^T (\frac{1}{2}|u(X_t^u, t)|^2 + f(X_t^u, t)) dt + g(X_T^u) + \int_0^T \langle u(X_t^u, t), dB_t \rangle,$$

while the gradients of the Continuous Adjoint loss with STL can be regarded as the gradient:

$$\mathcal{L}(u; X^u) := \int_0^T (\frac{1}{2}|u(X_t^u, t)|^2 + f(X_t^u, t)) dt + g(X_T^u) + \int_0^T \langle \text{stopgrad}(u)(X_t^u, t), dB_t \rangle,$$

That is, while we backpropagate through the stochastic integral, we do not take gradients with respect to the explicit evaluations of  $u$ .

- The Continuous Adjoint and Adjoint Matching losses without STL perform similarly, and they also perform similarly with STL (and slightly better than without STL). This contrasts with the behavior observed by [Domingo-Enrich et al. 2024](#), Tab. 2, where Adjoint Matching clearly outperforms the Continuous Adjoint method, arguably thanks to a lower gradient variance.

[Figure 4](#) and [Figure 5](#) show control  $L^2$  error curves for several kinds of SOCM-based algorithms. We use different terms when labeling the algorithms:

- The term  $M_t = I$  means that the reparameterization matrices  $M$  have not been trained and simply been set to the identity.
- The term *Diag.* means that the reparameterization matrices  $M$  have been parameterized as diagonal matrices. This allows to save memory and time at the expense of a less expressive model.
- The term *Scalar* means that the reparameterization matrices  $M$  have been parameterized as scalar multiples of the identity matrix. This allows to save memory and time at the expense of a less expressive model.
- The term  $M_t(T) = 0$  means that the architecture of the reparameterization matrices enforces that they are equal to zero at the terminal time  $T$ . This choice makes it possible to handle non-differentiable terminal costs  $g$  (although all the terminal costs in our examples are differentiable). See the code for more details on the architecture.

We make the following observations about [Figure 4](#):

- When it converges, Unweighted SOCM converges at the fastest rate in all setting in which it converges, but it fails to converge in the Double Well hard setting. This is consistent with the fact that Unweighted SOCM may not have the optimal control as the unique critical point ([Prop. 3](#)).
- Unweighted SOCM Diag.  $M_t(T) = 0$  performs very poorly, which is expected because it does not use any information about the terminal cost  $g$ , which means that it cannot converge to the optimal control.
- SOCM performs similarly to Unweighted SOCM in the Quadratic OU easy, Double Well easy and Linear settings, but quite differently in the other two. In the Quadratic OU hard setting, SOCM takes significantly longer to converge, because early on the importance weight  $\alpha$  has a lot of variance and the gradient is very noisy. In the Double Well hard setting, SOCM is the best method, but Unweighted SOCM fails to converge. Hence, we conclude that SOCM struggles with high cost values, while Unweighted SOCM struggles with multimodality.

- The Scalar, Diag. and  $M_t = I$  versions perform worse than the standard one, in general.
- SOCM-Adjoint performs worse than SOCM in general.

We make the following observations about [Figure 5](#):

- SOCM-Work tends to perform a bit better than SOCM-Cost, except for the Quadratic OU easy setting, where both achieve low error and SOCM-Cost is slightly better. This observation is consistent with Adjoint Matching (which has the same gradient in expectation as SOCM-Work) performing better than Continuous Adjoint (which has the same gradient in expectation as SOCM-Cost).
- While taking diagonal reparameterization matrices does not cause a significant performance drop in most cases (except for SOCM-Work in the Linear OU setting), enforcing  $M_t(T) = 0$  does yield higher control  $L^2$  errors.

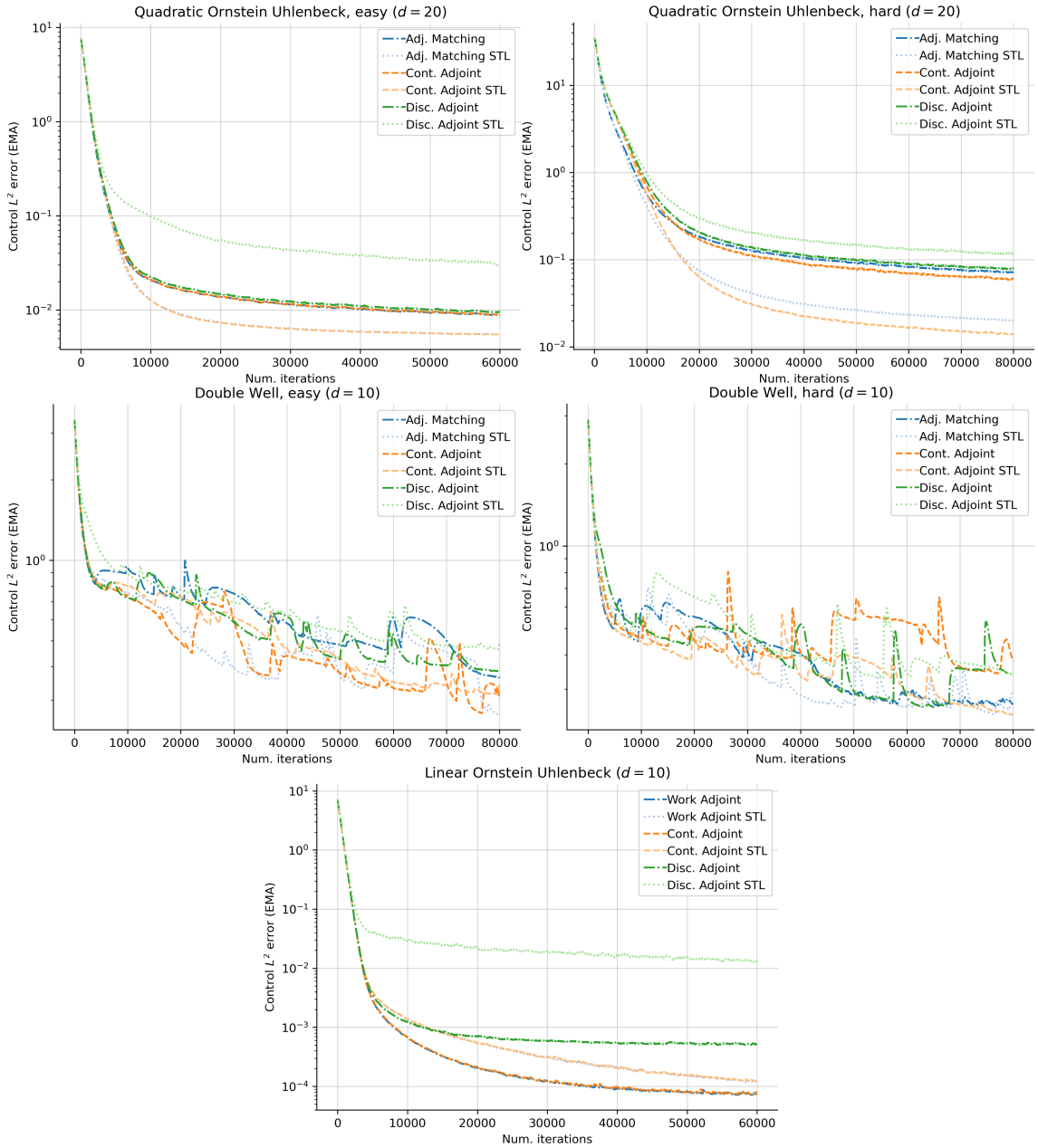


Figure 3: Control  $L^2$  error incurred by the Adjoint Matching, Continuous Adjoint and Discrete Adjoint losses (with and without the Sticking The Landing trick), on five different settings.

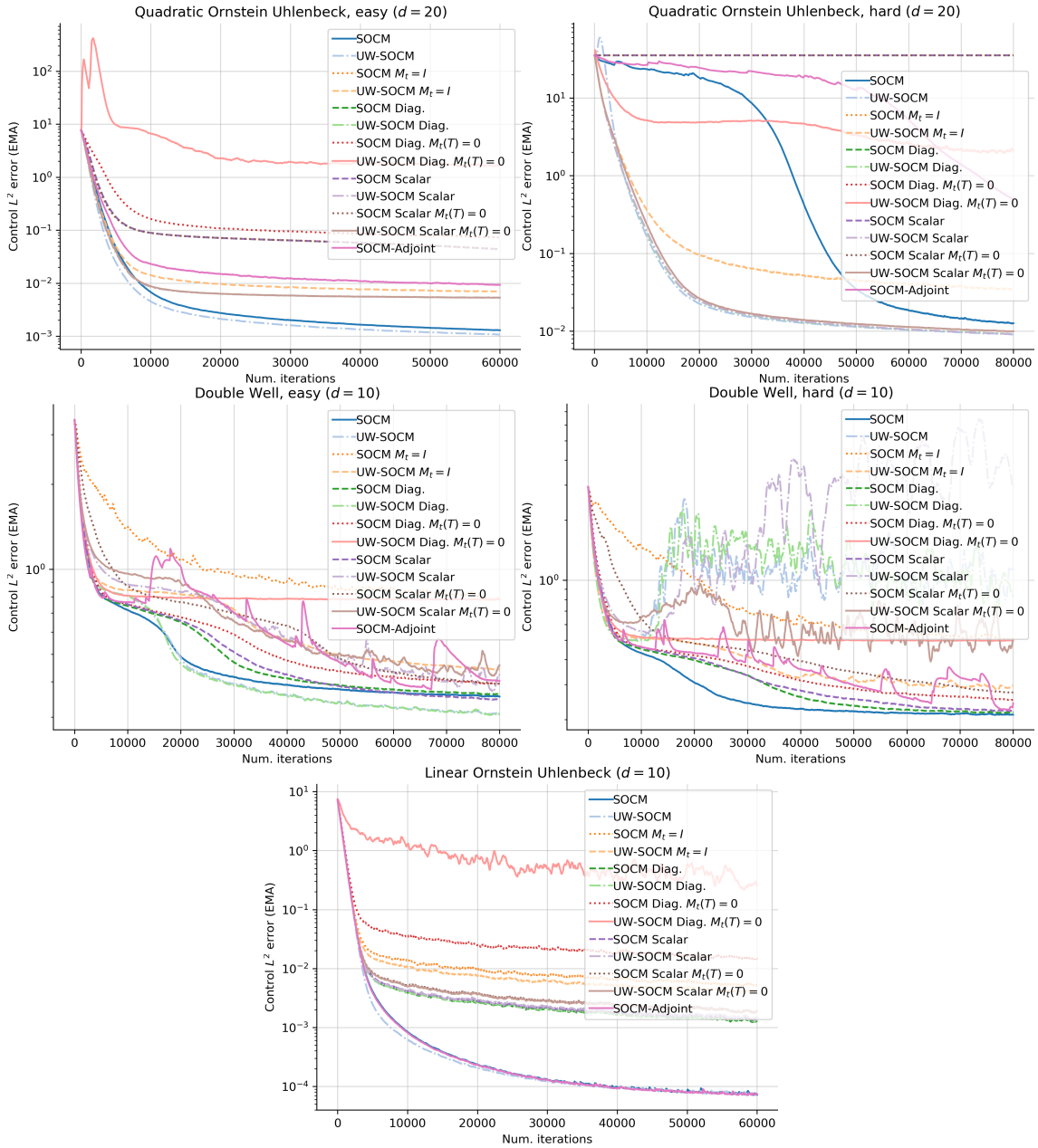


Figure 4: Control  $L^2$  error incurred by each loss function throughout training, on five different settings.

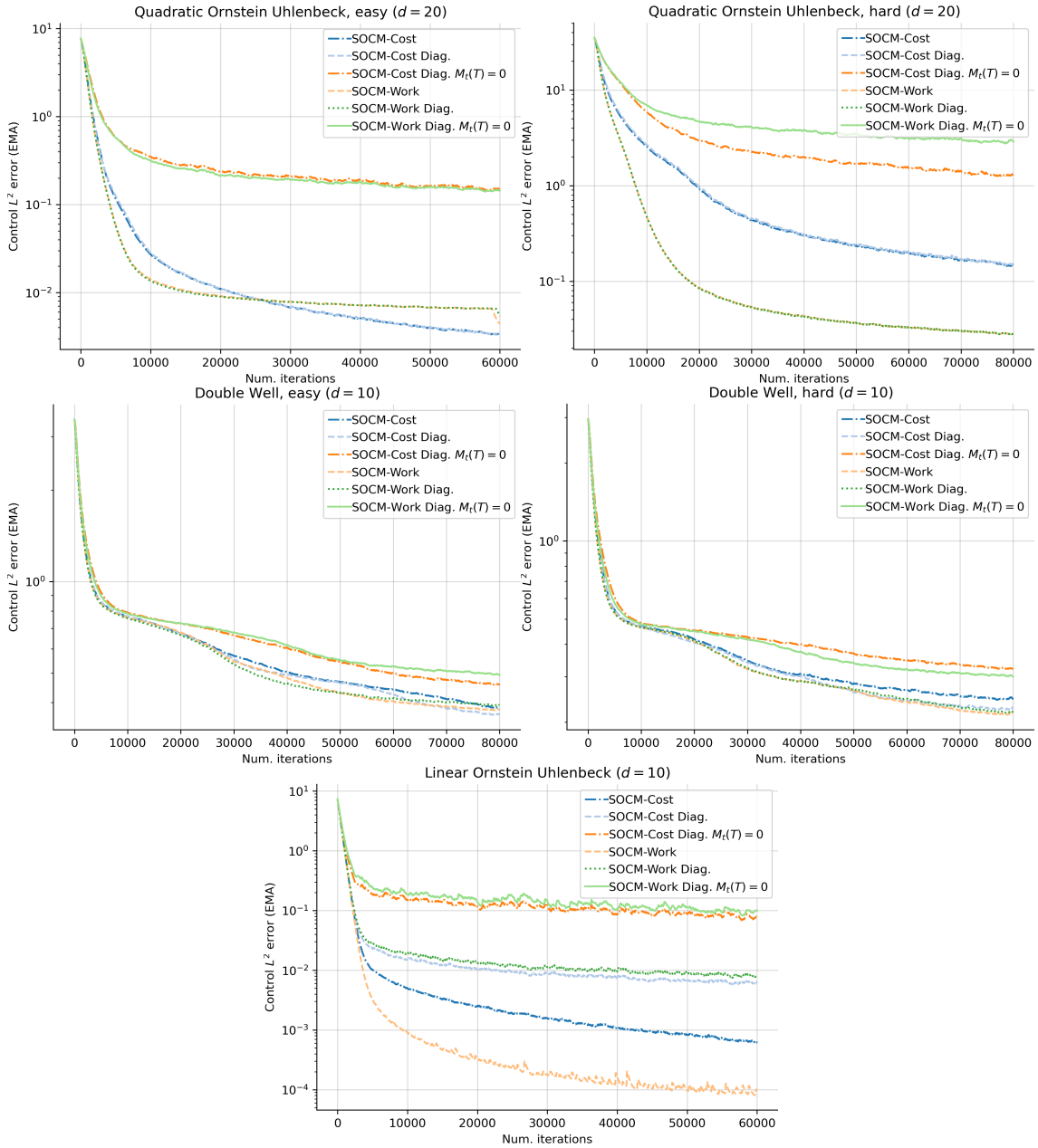


Figure 5: Control  $L^2$  error incurred by each loss function throughout training, on five different settings.